Results in Engineering 27 (2025) 106458

Contents lists available at ScienceDirect

Results in Engineering

journal homepage: www.sciencedirect.com/journal/results-in-engineering

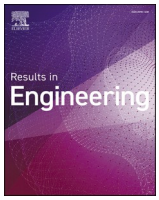

Research paper

Performance and emission analysis of CI engine fueled with *Dunaliella salina* biodiesel and TiO_2 nanoparticle additives: Experimental and ANN-based Predictive Approach

V Hariram [a,*], S Balamurugan [b], R Mohan [c], R Karthick [d], Nandagopal Kaliappan [e,i,*], K Barathiraja [f], J Godwin John [g], K Kamakshi Priya [h]

[a] *Department of Mechanical Engg, Hindustan Institute of Technology and Science, Chennai, Tamil Nadu, India*
[b] *Department of Mechanical Engg, Chennai Institute of Technology, Kundrathur, Tamil Nadu, India*
[c] *Department of Mechanical Engg, Sona College of Technology, Salem, Tamil Nadu, India*
[d] *Department of Mechanical Engg, M. Kumaraswamy College of Engineering, Karur, Tamil Nadu, India*
[e] *Department of Mechanical Engineering, Haramaya Institute of Technology, Haramaya University, Dire Dawa, Ethiopia*
[f] *Department of Mechanical Engg. Loyola Institute of Technology, Chennai, Tamil Nadu, India*
[g] *School of Automobile Engineering, Symbiosis Skills & Professional University, Kiwale, Pune, India*
[h] *Department of Physics, Saveetha School of Engineering, Saveetha University, SIMATS, Chennai, Tamil Nadu, India*
[i] *Department of Food Technology, Dhanalakshmi Srinivasan College of Engineering, Coimbatore, Tamilnadu, India*

ARTICLE INFO

Keywords:
Dunaliella salina
Artificial neural network
Soxhlet extraction
Transesterification
Sensitivity analysis
Techno-economic analysis
Engine performance

ABSTRACT

Growing demand for sustainable and renewable energy sources has intensified research into alternative fuels. *Dunaliella salina*, a green microalga, presents a promising feedstock for biodiesel production owing to its high oil yield and adaptability to extreme saline environments. This study aims to optimize the biodiesel production process and evaluate its feasibility in compression ignition (CI) engine applications. The algal oil was extracted from *Dunaliella salina* using the Soxhlet extraction technique and subsequently converted into biodiesel through a single-stage transesterification process using NaOH as a catalyst and methanol as the esterifying agent. The optimal reaction conditions - molar ratio of 1:8, catalyst concentration of 0.75 % by weight, and reaction temperature of 85 °C were identified. Gas Chromatography-Mass Spectrometry and Fourier Transform Infrared Spectroscopy analyses confirmed the presence of Linolenic acid and Arachidic acid in significant proportions. To enhance combustion characteristics and reduce emissions, biodiesel-diesel blends were evaluated in the presence of oxygenated titanium dioxide (TiO_2) nanoparticles at various compression ratios. An Artificial Neural Network (ANN) model was developed using the Levenberg-Marquardt algorithm, incorporating 27 datasets generated through a Response Surface Methodology (RSM)-based D-optimal design to predict engine performance and emission characteristics. Experimental results identified the D80DuBD20TiO_2 blend at a compression ratio of 18 (CR18) as optimal, demonstrating improved combustion efficiency and reduced emissions. The developed ANN model exhibited high predictive accuracy, with correlation coefficients (R) of 0.998, 0.993, and 0.996 for training, validation, and testing datasets, respectively. The techno-economic analysis assessed the Return on Investment and Operating cost of this investigation.

1. Introduction

Due to rapid urbanization across the globe, a significant surge in energy demand was witnessed leading to increased consumption of available fossil fuel. As time goes by, a steep decline in the petroleum based fuel was ascertained by the global population. In order to meet the demands which was at an alarming rate, researchers started focusing on the renewable, non-toxic, bio-degradable, non-edible and easily available substitute to cater the energy needs. Biodiesel is one such second generation alternative which can compromise the petro-diesel energy to a sizable amount. Biodiesel can be extracted from non-edible feedstock's like Jatropha, Pongamia, Karanja, Neem, Mahua etc. which may led to

* Corresponding authors.
E-mail addresses: connect2hariram@gmail.com (V. Hariram), nand204@gmail.com (N. Kaliappan).

https://doi.org/10.1016/j.rineng.2025.106458
Received 19 April 2025; Received in revised form 3 July 2025; Accepted 23 July 2025
Available online 25 July 2025

difficulties in scarcity in cultivable land areas [1]. Third generation biofuels overcome the hindrance caused by the vegetable based bio-fuel to a great extent thereby showing a pathway for promising future to energy demands. Biodiesel from micro-organisms (algae) is one such biofuel which can act as a suitable alternative for vegetable based fuel. Numerous eukaryotic and prokaryotic algal species like Chlorella sp., Spirogyra sp., Scenedesmus sp., Cylindrotheca sp., etc. produces prominent quantity of lipid during their life cycle which can be extracted by thermo-chemical methods for its usage as biofuel [2]. They utilize sunlight and micro-nutrients like the aquatic plants to produce lipid and carbohydrates in limited land area. Micro-lipids can be extracted through microwave heating, pyrolysis, distillation and chemical solvent extraction techniques as reported. Studies also suggest that algal based biodiesel in compression ignition (CI) engine in blended form, considerably reduces the formation smoke, Oxides of nitrogen (NO_x) and unburned hydrocarbon (UBHC), thereby also contributing to the greenhouse effect [3].

Recent advancements in combustible engines technologies enhanced their adaptability to hybrid fuel systems offering economical sustainability and are greener in operation. Vellaiyan et al. [4] blended ZnS/Cu, a nano composite with algal biodiesel at optimum levels and fueled the CI engine. They have cultivated *Chlorella vulgaris* using diluted waste water. Response Surface Methodology (RSM) was employed to examine the optimal performance of the engine with blended nano-composites as test fuel and its influence on fuel modification on the emission and performance parameters were also assessed. Adib et al. [5] employed a quasi-dimensional multi-zone combustion model to examine the CI engine fueled with *C. cohnil* biodiesel and validated numerically using Grey based Taguchi method. The optimization factors considered were S/N ratio, grey analysis and ANOVA statistical outcomes to address the efficacy of the compression ignition engine. D70MB30 fuel blends showcased higher NO_x and CO_2 with a significant decrement in smoke and PM emissions whereas BTE was similar across all fuel blends. Rashd et al. [6] addressed the thermodynamic and kinetic behavior during the synthesis of biodiesel through Soxhlet extraction technique of *Scenedesmus parvus* algal oil. The operating parameters were extraction temperature, extraction period, and S/L ratio. Higher algal oil yield was observed at 70 °C, 1:10 and 8 hrs of extraction temperature, S/L ratio and extraction period respectively.

Kattimani et al. [7] investigated the blends of fish oil methyl ester with diesel between 20 % and 80 % at 16.5, 17.5 and 18.5:1 compression ratio of a CI engine. The fuel injection operating parameters was varied between 240 and 260 bar. Improved BTE was noticed at 260 bar injection pressure for a 4 hole, 0.25 mm diameter fuel injector operating at 17.5:1 compression ratio when fueled with B40D60 blend ratio. The combined effect of EGR and CR in a CI engine was investigated by Rao et al. [8]. Novel Palmyra biodiesel was blended with neat diesel at 10, 20 and 30 % for fueling the test engine at compression ratio 16:1, 18:1 and 20:1 to understand its effect. POME 20 % fuel blend exhibited 6.91 % higher BTE with 10.2 % reduction in BSFC. 10 % EGR inducted along with POME 20 % fuel blend showcased a reduction of NO_x emission by 23 %. Santhosh et al. [9] studied the effect of cotton seed biodiesel in CI engine at variable compression ratio. It was noticed that BTE was significantly escalated with increase in NO_x across all operating conditions. Damodharan et al. [10] attempted to use waste plastic oil extracted through pyrolysis reaction in a CI engine at variable injection timing (21°, 23° and 25°, bTDC) in the presence of EGR. NO_x and Smoke was increased by 38 % and 46 % respectively at full load condition at 10 % EGR inductance.

Prediction based analysis tools were used to determine the benchmark values. Patnaik et al. [11] employed Artificial Neural Networks to study the emission and performance characteristics of waste cooking oil biodiesel fueled CI engine. The sensitivity analysis quantified the input parameters for predicting the output parameters and the correlation co-efficient, MSE, RMSE, R-all, MAP etc. were analyzed. The developed ANN model meticulously predicted the emission and performance parameters including the high correlation co-efficient value and lower MSE value of BTE as 0.9938 and 0.0397 respectively. Hosseini et al. [12] developed a standard back propagation ANN based algorithm to evaluate the vibration, performance and emission parameters of a CI engine fueled with alumina nano catalyst blended diesel-biodiesel fuel. They have employed the multi-layer perception network (MLP) for the non-linear mapping. The operating input parameters were the fuel properties and EGT, whereas the output factor were the engine vibration and exhaust emissions. Javed et al. [13] developed an ANN model to predict the Jatropha biodiesel fueled CI engine on its emission and performance phenomenon using trainlm back propagation algorithm with tan-sig and log-sig functions. Okonkwo et al. [14] predicted the performance parameters of a CI engine fueled with blends of *Chrysobalanus icaco* biodiesel using ANOVA techniques. They noticed that optimal blend ratio exhibited a root mean square and MAE values of 1.3723 and 0.650 respectively. Sekar et al. [15] prepared a hybrid fuel with blends of *Chlorella vulgaris* biodiesel, diesel and nano-particle along with the inductance of biogas. They noticed that infusion of nanoparticle decreased the BSFC considerably by 14.2 % at high loads. Mohammadhassani [16] employed ant colony optimization technique using ANN approach to predict the exhaust emission of an CI engine. The input parameters were fuel injection rate, air temperature, engine speed and power and the output factors were soot and NO_x. In order to improve system performance, optimization has emerged as a major area of investigation. These days, meta-heuristic and evolutionary algorithms that drew inspiration from mathematics and nature are used to supplement more conventional techniques like linear and nonlinear programming in assessing the performance of compression ignition engine [17]. For industrial heat transfer applications, precise thermal conductivity prediction of nanofluids is essential [18]. Because they disregard ingredient and environmental aspects, traditional models are unreliable. In this work, a hybrid AI model (LSSVM-ISA) trained on 1800 data points and optimized by enhanced simulated annealing. The model is very good at forecasting the thermal conductivity of nanofluids because it is more accurate and robust than empirical models and other AI techniques [19]

Studying engine performance through experiments is highly valuable to researchers worldwide, but it comes with several challenges. These include the need for skilled labor, complexities in managing the combustion setup, high fuel consumption, and issues with repeatability that can lead to longer testing times and material waste. Additionally, the exhaust emissions, particularly particulate matter (PM) and nitrogen oxides (NOx) pose serious risks to both human health and environment. In addition, the time-consuming experiential runs become more expensive with limited accuracy. Computer based prediction tools like ANN, GA and machine learning approaches gives a support hand in overcoming the hurdles of traditional practices by predicting the engine behavior to a great extent with less time duration. The predicted engine models can be optimized further using genetic algorithm and machine learning and other statistical tools to make it robust and highly reliable [20].

Despite extensive research on freshwater and marine microalgae such as *C. cohnil, Chlorella vulgaris, Scenedesmus* sp.*, Spirogyra* sp.*, and Cylindrotheca sp.*, relatively few studies have explored the potential of *Dunaliella salina* as a supplementary fuel in compression ignition (CI) engines alongside conventional diesel. This study focuses on the cultivation and extraction of algal oil in the form of lipids from *Dunaliella salina* under controlled aseptic laboratory conditions. The extracted algal oil was converted into biodiesel through a single-stage transesterification process using NaOH as a catalyst and methanol as the esterifying agent. The resulting biodiesel was subsequently characterized using advanced spectroscopic techniques to assess its fuel properties. To evaluate engine performance and emissions, an Artificial Neural Network (ANN)-based predictive model was developed to forecast the behavior of *Dunaliella salina* biodiesel-diesel blends in the presence of oxygenated nanoparticle additives. The predicted results were further

validated against experimental data, providing insights into the feasibility of *Dunaliella salina* biodiesel as a sustainable alternative fuel for CI engines.

2. Materials and methods

Dunaliella salina, a green unicellular microalga belonging to the division, class, order, genes and species of Chlorophyta, Chlorophycae, Chlamydononas, Dunaliella and *Dunaliella salina* respectively. It was found abundantly in saline environment with lipids and carotenoids in copious proportion. The sample of *Dunaliella salina* strains was procured from NCIM (National Collection of Industrial Microorganism), Pune, Maharashtra, India. f/2 nutrient medium was used to cultivate the micro-algae in the lab environment under aseptic acidic condition. 6 erlenmeyer flask were filled with 250 ml of f/2 nutrient solution along with stock solution and trace vitamins and metal mixtures in an amalgamation form. The microalgal strain were then implanted inside the erlenmeyer flask in nitrogen deficit condition. Carbon-di-oxide gas was allowed to circulate continuously with temperature of the environment maintained between 25 $^{\circ}C \pm 2$ °C. The complete growth stage of *Dunaliella salina* was achieved within 76 hrs of implant after which they were carefully harvested for lyophilization and pelleting. Water use is low at the lab scale and does not correspond to increased productivity. Therefore, we use scaled numbers from the literature to estimate net water use per kilogram of biodiesel. It can be seen that Net water consumption may be around 3–7 m^3/ kg biodiesel, freshwater use may be negligible, unlike terrestrial crops, environmental benefit may be seen as it reduces freshwater competition with agriculture [21,22].

Soxhlet extraction technique was adopted to extract the algal oil from *Dunaliella salina* microalgae. 50 g of harvested and pelleted microalgae was filled in the thimble and placed inside the central cartridge of the Soxhlet apparatus. The round bottomed flask of the Soxhlet apparatus was filled with 250 ml of *n*-hexane solvent and heated up-to 90 °C during which it changed its state to gaseous form and occupied the upper stem of the extractor. Upon cooling, the *n*-hexane solvent was condensed and reached the central cartridge containing the algal pellet and ruptured the cell wall membrane, thereby separating the lipid and dropping down them along with the condensed *n*-hexane. Repetition of this cycle 8 times collected 23 ml of algal oil in a single batch. Multiple (17) batch extracted 675 ml of *Dunaliella salina* bio-oil. The extracted algal oil was washed with double distilled water twice and heated up-to 100 °C for the removal of moisture content [23].

2.1. Transesterification of Dunaliella salina bio-oil

The FFA (Free Fatty acid) content of the *Dunaliella salina* bio-oil was found to be 1.92 through titration method using phenolphthalein. Therefore, single stage transesterification using sodium hydroxide and methanol was carried out to esterify the *Dunaliella salina* bio-oil. The conversion of triglycerides to FAME's was initiated at an optimum condition by maintaining the molar ratio as 1:8, catalyst concentration (NaOH) as 0.75 % by weight, 85 °C as reaction temperature and 110 min as reaction time period as suggested by Hosseini et al. [12] and El-Adawy et al. [24] using ANN approach. Initially, sodium methoxide solution was prepared by blending 1.3 g of sodium hydroxide in 100 ml of methanol solvent in a flat bottomed conical flask at agitation speed of 350 rpm for 25 min. Thereafter, 150 ml of extracted algal oil was thoroughly mixed with sodium methoxide solution at molar ratio of 1:6 and the agitation speed was raised up-to 450 rpm for 60 min at 65 °C for the esterification reaction to happen. Further, the mixture was transferred into an inverted separation funnel and a cooling period of 120 min was allowed during which a separation ring formation took place distinctly layering the glycerol and transesterified algal biodiesel. The esterified biodiesel was thoroughly mixed with 5 ml of acetone and heated up-to 70 °C for the removal of excess methanol, trace elements and moisture. Repeating the entire process in 8 batches yielded 485 ml of *Dunaliella salina* biodiesel with an esterification efficiency of 91.2 %. The extracted *Dunaliella salina* biodiesel and its processing are shown in Fig. 1.

Fig. 2

2.2. ANN approach

A machine learning technique, artificial neural network (ANN) was employed to model 2 different analyses. One is to understand the transesterification process and the other is to understand the emission and performance characteristics of diesel engine fuelled with both diesel and biodiesel. The experiments were designed by using response surface methodology-based D-optimal design. The total of 21 data set was collected from the experimentation with the operating parameters of load and various fuel and employed in ANN and shown in Table 9 and 10. MATLAB® 2020a software was used to develop the ANN model by utilizing Levenberg-Marquardt (LM) algorithm due to its ability to reduce the combination of squared errors, weights and determine the best combination that allows the network to generalize effectively. The developed ANN model with the three layers, such as input, hidden, and output layers respectively. The selected transfer functions for the both hidden layer and output layer were sigmoidal (tansig) and linear respectively. In the developed model, the network describes the number of neurons in the input and output layer with respect to the input parameters and output responses and the number of neurons in the hidden layers. Based on the performance, the number of neurons in the hidden layer has been evaluated. After the evaluation, the best neuron numbers have been observed and the selected network was considered for the present study. Eqs. (8–11) were used to estimate the errors observed from the developed ANN model [22].

$$2\left(n_{i/p}+n_{o/p}\right) \le n_h \le \frac{n_a\left(n_{i/p}+n_{o/p}\right)-n_{o/p}}{n_{i/p}+n_{o/p}+1} \tag{8}$$

$$MAE = \sum_{n_{i/p}=1}^{n_a} \left|\left(y_{i/p}-\widehat{y}_{i/p}\right)\right| \Big/ n_a \tag{9}$$

$$MAPE = \frac{100}{n_a}\sum_{n_{i/p}=1}^{n_a}\left(\left|y_{i/p}-\widehat{y}_{i/p}\right| \Big/ n_a\right) \tag{10}$$

$$RMSE = \sqrt{\sum_{n_{i/p}=1}^{n_a}\left(\left|\widehat{y}_{i/p}-y_{i/p}\right|\right)^2} \Big/ n_a \tag{11}$$

Where, $n_{i/p}$ – no. of neurons in the input layer, $n_{o/p}$ – no. of neurons in the output layer, n_h – no. of neurons in the hidden layer, n_a – no. of available data, MAE – mean absolute error, MAPE – mean absolute percentage error, and RMSE - root mean square error.

The study observed that increasing the methanol-to-oil molar ratio from 1:4 to 1:6 improved biodiesel yield, with a peak yield of 91.2 wt % at 1:6, due to enhanced conversion of oil to esters. Further increase beyond 1:6 reduced yield, likely due to equilibrium imbalance. The optimal catalyst concentration was found to be 0.75 wt %, as higher concentrations led to soap formation via saponification, reducing yield. A reaction time of 110 min was optimal; extending it further showed marginal improvement or slight deterioration in yield and fuel properties. An Artificial Neural Network (ANN) model using a Bayesian-based algorithm was employed to validate experimental biodiesel yield. Key process variables were selected from studies analyzed, and an optimized architectural design was identified as the most effective for yield prediction. The model demonstrated high predictive accuracy with statistical indicators such as $R = 0.97709$, $R^2 = 0.98214$, and RMSE = 0.37489, closely aligning with regression results. The ANN effectively captured the relationship between input parameters and yield, with predicted values closely matching experimental data as shown in Table 1. Similar outcomes were achieved by Pai et al. [25] and Alzubaidi

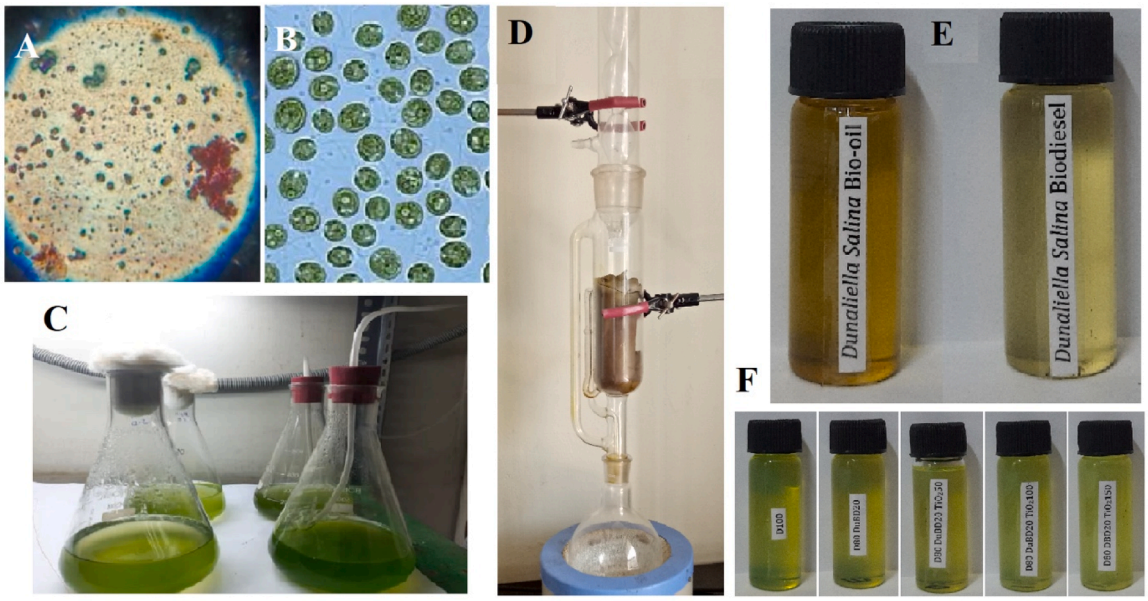

Fig. 1. Microscopic view of Dunillia salina (A & B), Algal oil extraction (C & D), Biodiesel and Test fuels (E & F).

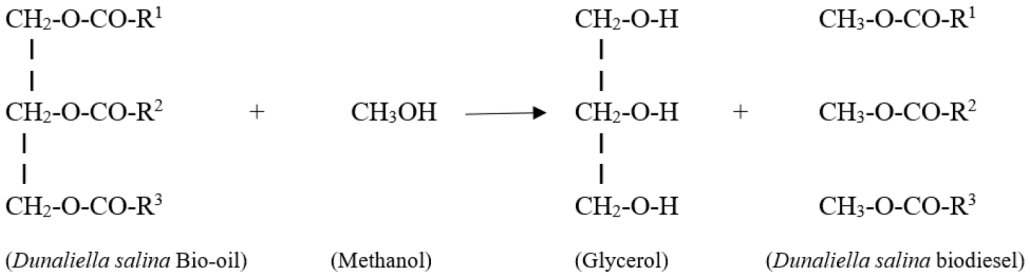

Fig. 2. Transesterification reaction - Dunaliella salina bio-oil to Biodiesel.

et al. [26] in their investigation.

Table 2

2.3. Synthesis of TiO_2 nano-particle

Titanium di-oxide (TiO_2) nanoparticle was synthesized in the Center of Clean Energy and Nano Convergence (CENCON), HITS, Padur campus, Chennai. Titanium tetra isopropoxide was used as the base material for the synthesis of TiO_2 nano-particle through Sol-gel technique. Hydrochloric acid, ethanol and H_2O in de-ionized form were used to prepare the TiO_2 nano-particle. Initially, 10 g of Titanium tetra isopropoxide was thoroughly mixed with 15 ml of ethanol and hydrochloric acid and stirred continuously for 45 min. Further, 10 ml of de-ionized H_2O was blended with the mixture and continued stirring for 90 min at ambient temperature and the pH value was maintained at 5. Titration process of the resultant mixture with de-ionized H_2O formed a gel like substance which on calcination at 180 °C for 6 h produced TiO_2 nano-particle. TiO_2 nano-particle was characterized using EDS (Energy Dispersive X-Ray spectroscopy, Make - Bruker S_2 Puma Series). TiO_2 cubic structure was observed at the various lattice plane with their corresponding diffraction peaks and was in accordance with the International Centre for Diffraction Data (ICDD). Scherer's equation was employed to evaluate the crystalline structure of TiO_2 as in Eq. (1) [27–38]

$$D = (0.89\lambda)/(\beta Cos\theta) \quad (1)$$

Where D is the Scherer's constant, λ is X-ray diffraction wavelength, β is the full width angle and θ denotes the Brass's angle.

The obtained dispersive spectrum exhibits the presence of oxygen and titanium elements with noteworthy fringes at the edges of cubic structured TiO_2 nano-particle along with negligible agglomerations. Although technically feasible, scalability is constrained by expensive, hazardous chemicals and high energy requirements. Green synthesis, solvent recycling, and energy-efficient procedures can all help to lessen the substantial environmental impact that life cycle studies show. A thorough LCA that takes energy sources, recycling, and precursor substitutes into account is necessary for further scale-up, hence considering the literature study [29–36] TiO_2 was employed. The particle size of TiO_2 was monitored using Dynamic Light Scattering method. 1 ml of derived nano-infused biodiesel sample was subjected to Quasi elastic light scattering arrangement to understand the Brownian movement. A laser light focusing on the *Dunaliella salina* biodiesel sample with a detector confirmed the nano size distribution and its homogeneity.

2.4. FTIR and GCMS characterization studies

Bruker Alpha Platinum attenuated Internal Reflectance Spectrometer was employed in this study to understand the *Dunaliella salina* biodiesel's transmittance. The equipment uses total internal reflection phenomenon with brazed tungsten carbide crystal and rock solid Micheleon interferometer through single reflection module to examine the transmittance range of biodiesel sample along with deurated triglycime sulphate as detector. The angle of incidence was produced by a crystal when the infrared light ray was made to pass through in-line with 1 ml of *Dunaliella salina* biodiesel sample. The instrument has a resolution of 2 cm^{-1} and spectral range between 500 cm^{-1} and 4000 cm^{-1}.

Table 1
Prediction of ANN biodiesel yield.

Trials	Molar Ratio in (v/v) Y1	Catalyst Conc. (wt %) Y2	Reaction Time (in min) Y3	Expt. Biodiesel Yield (%)	ANN Predicted yield (%)
1	1:4	0.75	70	83.7	84
2	1:4	0.75	90	84.4	84.7
3	1:4	0.75	110	84.9	85.2
4	1:4	0.90	70	84.4	84.7
5	1:4	0.90	90	85.5	85.8
6	1:4	0.90	110	86.2	86.5
7	1:4	1.05	70	84.6	84.9
8	1:4	1.05	90	86.3	86.6
9	1:4	1.05	110	88	88.3
10	1:6	0.75	70	87.2	87.5
11	1:6	0.75	90	88.3	88.6
12	1:6	0.75	110	91.2	91.5
13	1:6	0.90	70	85.7	86
14	1:6	0.90	90	88.8	89.1
15	1:6	0.90	110	89.9	90.2
16	1:6	1.05	70	88.3	88.6
17	1:6	1.05	90	89	89.3
18	1:6	1.05	110	90.2	90.5
19	1:8	0.75	70	87.9	88.2
20	1:8	0.75	90	90	90.3
21	1:8	0.75	110	90.8	91.1
22	1:8	0.90	70	87.4	87.7
23	1:8	0.90	90	89.3	89.6
24	1:8	0.90	110	90.9	91.2
25	1:8	1.05	70	86.2	86.5
26	1:8	1.05	90	87.4	87.7
27	1:8	1.05	110	89.4	89.7

Table 2
Properties of synthesized TiO_2.

Color	White
Purity	97.72 %
Average particle size	19 – 23 nm
Micro strain	0.083 ξ
Specific surface area	369 m2/kg
True density	0.18 g/cc

Fourier Transform Infra-red analysis was performed on the *Dunaliella salina* biodiesel using IR software. The system is employed with single reflection ATR interface on the sample with a surface penetration depth of 2 μm. From the FTIR transmittance, it could be noticed that there is a reactive shift from mono-alkyl ester group in the algal oil to fatty acid methyl ester group in the biodiesel sample, (i.e.) from (R_1—CoR) =*O*) to $R_1C(OCH_3)$ =*O*, where R_1 specifies the presence of long chain hydrocarbon in the algal oil and biodiesel as well. Prominent transformation peaks were seen at 1741.22 cm^{-1} and 2923.46 cm^{-1} of the *Dunaliella salina* biodiesel spectrum whereas *Dunaliella salina* bio-oil sample showed its highest peak at 1423.15 cm^{-1}. Cluster peaks between 1169.221 cm^{-1} and 1460.99 cm^{-1} denotes the presence of carboxylic acid and O—H derivatives [34–37]. The existence of saturated aldehydes was also noticed due to the peak at 2853.91 cm^{-1}. The detailed FTIR spectrum of *Dunaliella salina* biodiesel is shown in Fig. 3.

A single quadruple 5977B mass spectrometer (8890) GC system with thermal stabilization was employed to estimate and detect the presence of various fatty acid methyl esters in *Dunaliella salina* biodiesel sample. The GC system was equipped with an inlet split ratio of 7500:1 and SSL injector along with a pre-heated monolithic hyperbolic quadruple mass filter in electron and chemical impact ionization mode. The oven temperature can be increased up-to 450 °C whereas the ion source and quadruple temperature was varied between 150 °C-350 °C and 106 °C-200 °C respectively. GCMS analysis revealed the efficacy of transesterification process using NaOH and methanol solvents. The chromatogram in Fig. 4 shows numerous peaks at Retention time to the corresponding FAME's. The base peak at *m/z* 74 demonstrates the occurrence of McLafferty rearrangement process wherein the mono-alkyl ester in the algal oil was transformed into fatty acid methyl esters group in the *Dunaliella salina* biodiesel due to the loss of carboxyl and methoxy ions. The mass fragmentation exhibits β cleavage and redistribution of the hydrogen /carbon atoms resulting in multiple peak clusters [39]. The Table 3 shows the existence of various fatty acid methyl esters in the *Dunaliella salina* biodiesel sample with their corresponding retention times and composition wherein Linolenic acid was found to be available in abundant quantity followed by Arachidic acid.

As discussed, *Dunaliella salina* biodiesel was derived through single stage transesterification process using NaOH and methanol solvents. The physio-chemical properties like kinematic viscosity, density, heating

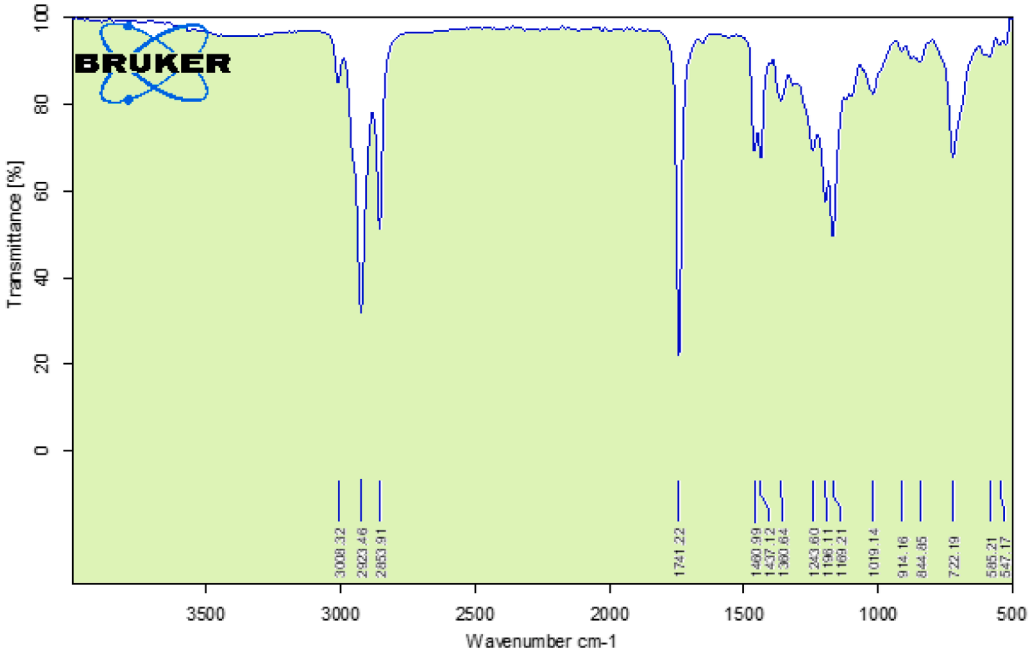

Fig. 3. FTIR Transmittance of *Dunillia salina* Bio-diesel.

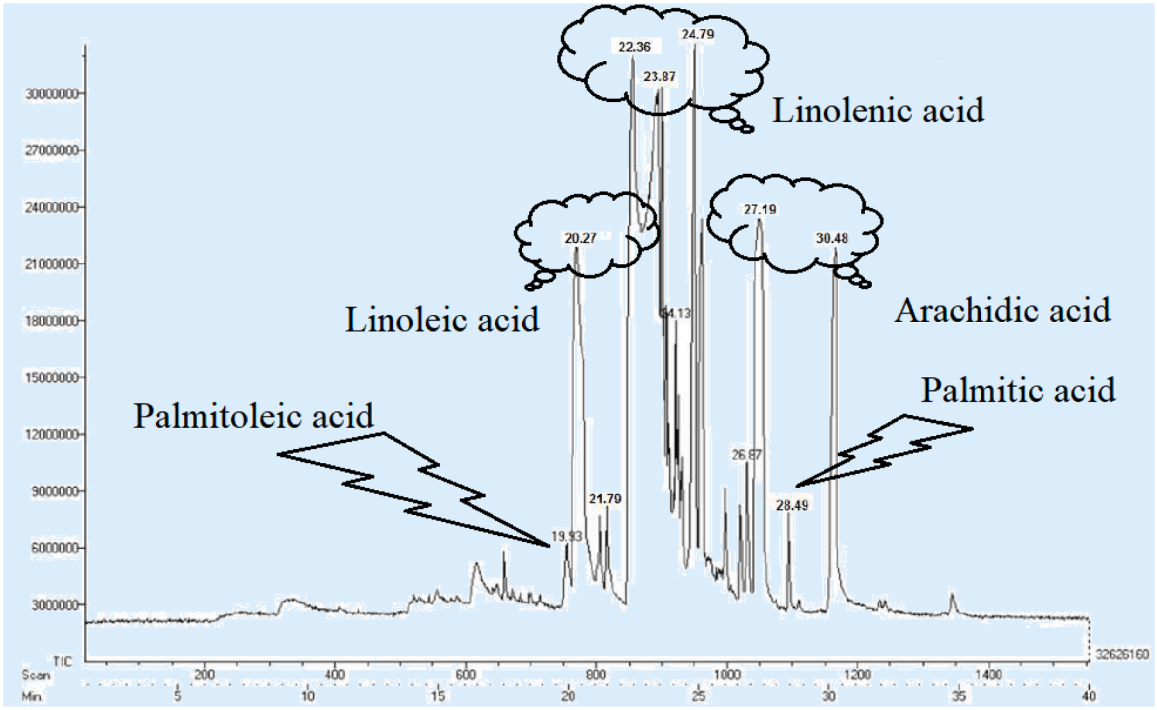

Fig. 4. GCMS Chromatogram of *Dunaliella salina* Bio-diesel.

Table 3
Fatty acid composition in *Dunaliella salina* biodiesel.

Retention time (RT)	Composition (%)	Fatty acid Systematic name	Fatty acid Common name
19.93	2.225	Hexadecenoic acid methyl ester	Palmitoleic acid
20.27	8.512	12-Octadecenoic acid methyl ester	Linoleic acid
21.79	0.412	Heptadecanoic acid methyl ester	Lauric acid
22.36	37.458	14–17 Octadecadienoic acid methyl ester	Linolenic acid
24.79	14.569	Eicosanoic acid methyl ester	Arachidic acid
27.19	6.879	Docosanoic acid methyl ester	Oleic acid
28.49	1.0254	Tricosanoic acid methyl ester	Palmitic acid
30.48	2.126	Tetracosanoic acid methy ester	Lignoceric acid

Saturated fatty acid: 23.784 %.
Unsaturated fatty acid: 71.254 %.
Unknown components: 4.962 %.

value, acid value, flash point and cetane number of *Dunaliella salina* bio-oil and its biodiesel were determined as per ASTM D6751 standards and tabulated in Table 4. The blending of *Dunaliella salina* biodiesel with neat diesel was carried out in volume proportions as 20 % blend ratio due to its universal acceptance with minimal or no modification in the existing compression ignition engine setup. Further, Neat diesel - *Dunaliella salina* biodiesel blend (D80DuBD20) was amalgamated with synthesized TiO_2 in three proportions, (i.e. 50 ppm, 100 ppm and 150 ppm) to evaluate the engine's behaviour when fuelled with oxygenated fuel additives in the performance and emission phenomenon. Infusing titanium di-oxide with diesel-biodiesel fuel blend improved the cetane number and kinematic viscosity significantly. The heating value of the test fuels also showed an upsurge with in TiO_2 concentration. Table 5 exhibited the physio-chemical properties of *Dunaliella salina* bio-oil and its biodiesel whereas the Table 5 compares the various test fuels blends employed in the present investigation.

Table 4
Physio-chemical properties of *Dunaliella salina* bio-oil and its biodiesel.

Properties	*Dunaliella salina* bio-oil	*Dunaliella salina* biodiesel	Neat Diesel	ASTM standards
Heating value (MJ/kg)	30.75	39.75	43.8	–
Kinematic Viscosity @ 40 °C (mm^2/s)	18.259	5.21	1.9 – 4.1	1.9 – 6.0
Density @ 15 °C (kg/m^3)	927	858	845	–
Acid value (mg KOH/g)	57.23	0.72	–	< 0.8
Cetane number	37	43	48	–
Cloud point (°C)	14	8	–	–
Flash point (°C)	182	189	67	> 130 °C

Table 5
Physio-chemical properties of test fuels.

Properties	D80DuBD20	D80DuBD20 $TiO_2$50	D80DuBD20 $TiO_2$100	D80DuBD20 $TiO_2$150
Density @ 15 °C (kg/m^3)	849	851	853	856
Kinematic Viscosity @ 40 °C (mm^2/s)	2.97	2.74	2.76	2.80
Heating value (MJ/kg)	40.83	41.32	42.02	42.97
Flash point (°C)	124	118	114	112
Cetane number	45	45.3	46	46.9

3. Experimentation

Kirloskar 240 PE, naturally aspirated, single cylinder, water cooled

compression ignition engine was employed in the present investigation to evaluate the performance and emission phenomenon of Neat diesel - *Dunaliella salina* biodiesel blend infused with TiO_2 nano-particle at variable compression ratio. The loading of the test engine was accomplished using a water cooled eddy current dynamometer. The engine's combustion, emission and performance data's were received as signals through the inlet-outlet temperature-pressure, rate heat discharge, flue flow measurement, calorimeter reading and others. Diesel fuel data was used a base reading across all loading condition whereas the engine was allowed to operate at the maximum load of 90 % (i.e.) upto 3.15 kW of the rated capacity. To maintain homogeneity of the experimental trials, neat diesel fuel was used in between the multiple test fuel blends as shown in the experimental test matrix in Table 6. Two different fuel canister were maintained at the top as shown where one was filled with neat diesel and the other with *Dunaliella salina* Biodiesel blend initially and interchanged with other test fuel blends as and when required. The time taken for 100 ml fuel consumption for each trials were recorded along with corresponding engine speed at all load using a crank angle encoder to evaluate the engine's performance. The exhaust tail pipe was fitted with probes from AVL444N-Five gas analyser to record the emissions like CO, UBHC, NO_x, CO_2 and AVL437C-Smoke meter for recording the smoke opacity. The variation in compression ratio was achieved employing a tilting block mechanism near the cylinder head without altering the geometry of piston and combustion chamber with minimal variation in the clearance volume. Employing this mechanism varied the compression ratio between 12 and 20, wherein the present investigation studied the effect of CR varied between 17 and 18 as recommended in the literature. Increasing CR beyond a certain point, requires stronger materials to withstand higher cylinder pressures and temperatures and may lead to engine knocking, mechanical wear, and thermal fatigue. The CR range between 17 and 18 is within the safe mechanical and thermal tolerance of most commercial diesel engines, avoiding the need for significant redesign. The detailed schematic of the test engine is shown in Fig. 5. Table 6 shows the complete test matrix performed in this experimental investigation and the significant outcomes of Neat diesel - *Dunaliella salina* biodiesel blend infused with TiO_2 nano-particle blends at variable CR are discussed further. The test engine specification of the test engine is shown in Table 7.

Table 6
Experimental test matrix.

Fuel types	Engine loading condition	Observation
Neat diesel at CR 17 Neat diesel at CR 17.5 Neat diesel at CR 18 Neat diesel (80 %) + *Dunaliella salina* biodiesel (20 %) at CR 17 Neat diesel (80 %) + *Dunaliella salina* biodiesel (20 %) at CR 17.5 Neat diesel (80 %) + *Dunaliella salina* biodiesel (20 %) at CR 18 Neat diesel (80 %) + *Dunaliella salina* biodiesel (20 %) + TiO_2 50 ppm at CR 17 Neat diesel (80 %) + *Dunaliella salina* biodiesel (20 %) + TiO_2 50 ppm at CR 17.5 Neat diesel (80 %) + *Dunaliella salina* biodiesel (20 %) + TiO_2 50 ppm at CR 18 Neat diesel (80 %) + *Dunaliella salina* biodiesel (20 %) + TiO_2 100 ppm at CR 17 Neat diesel (80 %) + *Dunaliella salina* biodiesel (20 %) + TiO_2 100 ppm at CR 17.5 Neat diesel (80 %) + *Dunaliella salina* biodiesel (20 %) + TiO_2 100 ppm at CR 18 Neat diesel (80 %) + *Dunaliella salina* biodiesel (20 %) + TiO_2 150 ppm at CR 17 Neat diesel (80 %) + *Dunaliella salina* biodiesel (20 %) + TiO_2 150 ppm at CR 17.5 Neat diesel (80 %) + *Dunaliella salina* biodiesel (20 %) + TiO_2 150 ppm at CR 18	At No load, Low load, Part load and full load operations	Base reading for comparison Evaluation of performance and emission phenomenon

Significant outcomes are highlighted and discussed further at variable Compression ratios (CR).

3.1. Uncertainty analysis

The variation between measured quantity and true value is termed as experimental uncertainty or error. Uncertainty may arise due to instrumentation, environmental aspect and human influencing factors. Therefore, it is essential to evaluate and eradicate the uncertainty and errors in the experimental trials to improve the accuracy of the present investigation. In multifaceted experimentation, error analysis is a vital stage which suitably initiates corrective actions to obtain most accurate data. Uncertainties and errors can be evaluated using instrumentation on the same or similar experiments repeatedly for several times. In the present investigation, root mean square technique as in Eq. (2–7) estimated the overall combined uncertainties. The accuracy, resolution and range of the various instrumentation employed in this study are tabulated in Table 8.

$$U_{BTE} = \sqrt{\left(U_{\omega}\, x\, \frac{BTE}{\omega}\right)^2 + \left(U_T\, x\, \frac{BTE}{T}\right)^2 + \left(U_{m_{fuel}}\, x\, \frac{BTE}{m_{fuel}}\right)^2} \quad (2)$$

$$U_{BSFC} = \sqrt{\left(U_{\omega}\, x\, \frac{BSFC}{\omega}\right)^2 + \left(U_T\, x\, \frac{BSFC}{T}\right)^2 + \left(U_{m_{fuel}}\, x\, \frac{BSFC}{m_{fuel}}\right)^2} \quad (3)$$

$$U_{CO=} \sqrt{\left(\frac{U_{CO}}{CO}\right)^2 + \left(\frac{U_{E_s}}{E_s}\right)^2} \quad (4)$$

$$U_{UBHC=} \sqrt{\left(\frac{U_{UBHC}}{UBHC}\right)^2 + \left(\frac{U_{E_s}}{E_s}\right)^2} \quad (5)$$

$$U_{NOx=} \sqrt{\left(\frac{U_{NOx}}{NOx}\right)^2 + \left(\frac{U_{E_s}}{E_s}\right)^2} \quad (6)$$

$$U_{Smoke=} \sqrt{\left(\frac{U_{Smoke}}{Smoke}\right)^2 + \left(\frac{U_{E_s}}{E_s}\right)^2} \quad (7)$$

Where U_{ω} is the internal energy, T is the outlet temperature, m_{fuel} is the mass of fuel particle

Each experiments were repeated three times (i.e. number of runs per condition) to satisfy the experimental repeatability. The error bar towards the uncertainty values for the performance and emission plots are displayed in Fig. 6.

The results obtained from the developed ANN model for training, validation, test, and all datasets respectively as shown in Fig. 2. The observed results showed a better coefficient of correlation for training,

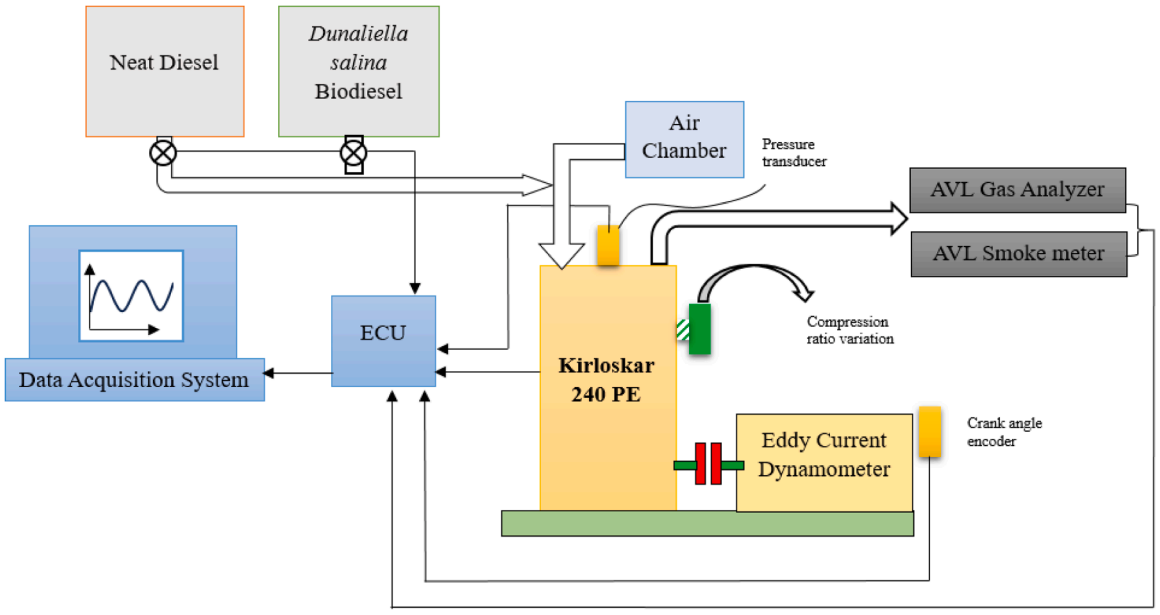

Fig. 5. Schematic diagram of Test engine.

Table 7
Test engine specification.

Test engine	Kirloskar 240 PE
Number of cylinder	One
Rated speed	1500 rpm
Rated power	3.5 kW
Fuel injection pressure	220 bar
Compression ratio	17.5 (Factory set) Variable between 12 and 20
Fuel injection timing	23°bTDC
Bore and Stroke length	87.5 and 110 mm
Number of spray nozzle	3
Angle of fuel spray	120°
Nozzle spray hole diameter	0.3 mm
Loading type	Eddy current dynamometer

Table 8
Uncertainty analysis.

Instrumentation	Measurement	Accuracy	Range	Uncertainty
Crank angle encoder	Crank angle	±1°	0 – 720°	± 0.03 %
AVL444N-Five gas analyser	CO	±0.4 %	0 – 10 %	±0.2 %
	CO_2	±0.5 %	0 – 20 %	±0.15 %
	NO_x	±40 ppm	0 – 5000 ppm	±0.5 %
	UBHC	±10 ppm	0 – 10,000 ppm	±0.2 %
AVL437C-Smoke meter	Soot	±1 %	0 – 100	±1.1 %
Temperature indicator	Temperature	±1 °C	0 – 800 °C	±0.3 %

validation, test, and all datasets respectively, and exposed that the developed ANN model is capable for predicting the best emission and performance characteristics of diesel engine fuelled with the biodiesel. Table 10 illustrates the predicted output responses (emission and performance characteristics) by utilizing developed ANN model, which predicts the results are very closer to the experimental results and authorizes that the developed ANN model is suitable to design the emission and performance characteristics of a diesel engine fuelled with biodiesel. Also, Table 10 displays the statistical results for the developed ANN model of the performance and emission characteristics of engine fuelled with biodiesel, expressed the variation between the experimental and

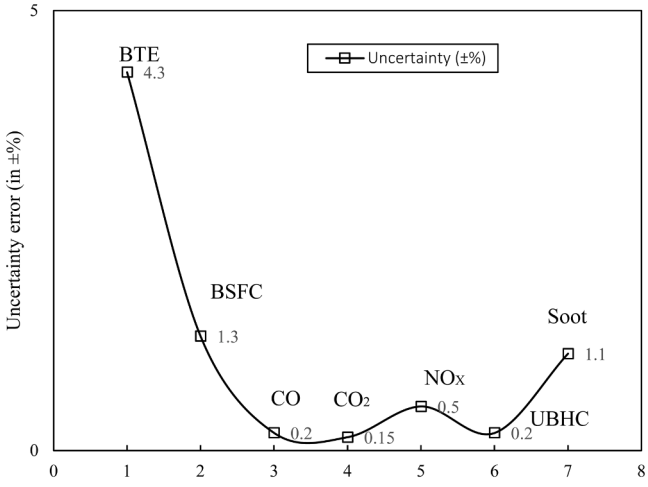

Fig. 6. Error Bar for Performance and Emission.

predicted results. These results showed that the values of MAE, MAPE, and RMSE are very closer to one. The developed ANN model displays a better capability to design and interpret the experimental results.

3.2. Sensitivity analysis

The effect of the input factors in the developed ANN model has been estimated by using the connection weights approach [40,41]. The connection weight was developed by using network architecture in MATLAB® 2020a software, though the relative impacts (RI) were generated by Eq. (12).

$$RI(\%) = \frac{\sum_{n_{ih}=1}^{n_h} C_{wt}}{\sum_{n_{ih}=1}^{n_h}\sum_{i=1}^{n_h} C_{wt}} X100 \quad (12)$$

Where C_{wt} - connection weight and n_{ih} - input - hidden layer neurons.

4. Results and discussion

Initially, experiments were conducted with neat diesel at the factory set compression ratio (17.5:1) on all loading conditions to understand

the engine's behavior on the performance and emission phenomenon. Further, neat diesel was volumetrically blended with *Dunaliella salina* biodiesel at ratios of 10 %, 20 %, 40 % and 60 % for fueling the CI engine. It was noticed that up-to 20 % of fuel blends, the engine was stable at all loads, but when the blend ratio was increased beyond 20 %, the engine showcased erratic behavior with variations in its performance which makes it essential to modify the factory setup. Therefore, 20 % fuel blend was standardized across all compression ratios and nano particle added D80DuBD20. In the present scenario, test run at CR18 showcased superior performance with minimal exhaust emission which pathway further studies to understand the effect of nano additive (TiO_2) at various compositions. The optimal prediction on the performance and emission phenomenon were carried out using RSM based D-optimal ANN approach as discussed above.

4.1. Brake thermal efficiency

Brake Thermal Efficiency (BTE) depicts the ratio between heat supplied to the quantity of developed brake power (Fig. 7). Variations in the BTE with respect to CR and nano-added fuel blends illustrates the engine adaptability and smooth functioning with superior performance. At CR17.5, neat diesel exhibited BTE of 35.87 % at full load condition, whereas D80DuBD20 fuel blend showed marginally lower BTE by 7.9 %. An increment and decrement in CR by 0.5 significantly varied the BTE upto 35.20 % and 32.48 % respectively. Establishing higher BTE at CR18, nano TiO_2 was infused at 50, 100 and 150 ppm to the diesel-biodiesel blend at CR18 which exhibited 36.5 %, 46.6 % and 43.25 % of BTE respectively whereas ANN predictions showcased a BTE of 36.40 %, 46.45 % and 43.10 %. It can be noticed that D80DuBD20$TiO_2$100 fuel blend showcased higher BTE at part and full load conditions upto 40.8 % and 46.6 % experimentally and 40.64 % and 46.45 using the ANN prediction model respectively. This may be due to escalated combustion chamber temperature, improvised fuel atomization and better mixing of air and fuel at part and full load operations. Liberation of additional oxygen due to micro-explosion at all load in CR18 with D80DuBD20TiO_2 may also be a reason for superior BTE.

4.2. Brake specific fuel consumption

Brake Specific Fuel Consumption (BSFC) is the measure of fuel consumed to produce unit power. Fig. 8 depicts the variation in BSFC for neat diesel at CR17.5, diesel-biodiesel blend at CR17, 17.5 and 18, diesel-biodiesel-nano fuel blends at CR18. For optimum performance of a CI engine, the BSFC should be as low as possible with increasing engine

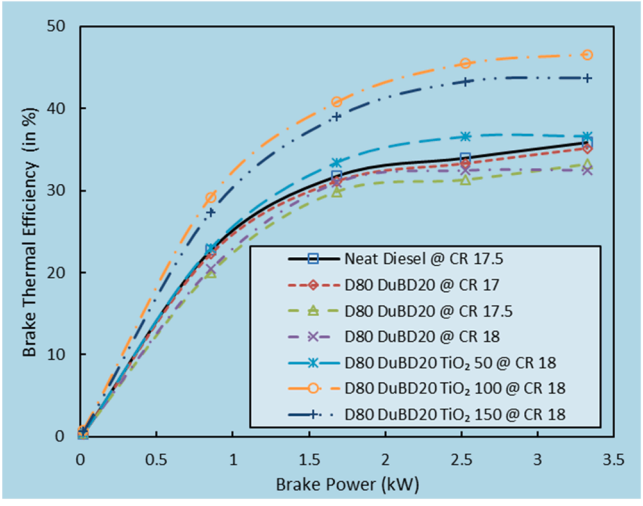

Fig. 7. Variation in Brake Thermal Efficiency at Compression ratio 17, 17.5 and 18.

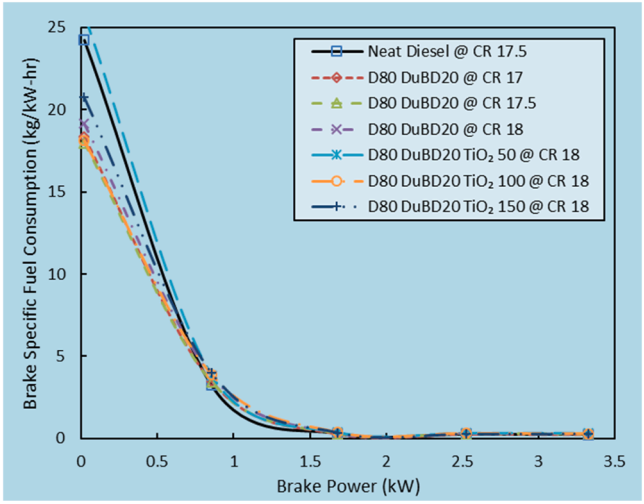

Fig. 8. Variation in Brake Specific Fuel Consumption at Compression ratio 17, 17.5 and 18.

load. The physical factor which affects the BSFC are fuel density, calorific value, cetane number, air/fuel mixture ratio and its miscibility. The developed ANN model also showcased the BSFC in a similar trend which was in-line with the experimental outcomes. From the Fig. 8, it can be observed that neat diesel at CR17.5 exhibited a higher BSFC of 24.23 kg/kWhr at low loading condition. Increase in the engine load significantly reduced the BSFC considerably. Diesel-*Dunaliella salina* biodiesel blend at CR17, 17.5 and 18 showcased lower BSFC between 18.34 kg/kWhr and 19.18 kg/kWhr at low loads. Addition of TiO_2 to the diesel-biodiesel blend upto 50 ppm increased the BSFC notably upto 6.044 %. Increasing the nano-particle concentration by another 50 ppm upto 100 ppm exhibited lower BSFC of 18.11 kg/kWhr, 0.36 kg/kWhr and 0.30 kg/kWhr for low, part and full load conditions wherein ANN predicted a similar BSFC of 18.07 kg/kWhr, 0.35 kg/kWhr and 0.31 kg/kWhr respectively. Increase in the CR had an important effect in decrementing the BSFC considerably across all loads for D80DuBD20 and its nano blends which may be due to prolonged time duration for better fuel atomization and mixing, enhanced progressive combustion phase and higher in-cylinder temperature [15]. D80DuBD20TiO_2 fuel blend showcased a significant decrease in the BSFC at CR18 which may be due to enhanced nano-particle dispersion and supplementation of additional oxygen atom during the micro-explosion of nano particle at higher combustion temperature and prolonged combustion duration.

4.3. Unburned hydrocarbon emission

Unburned Hydrocarbons are mainly formed due to incomplete and ineffective combustion in the CI engine. Fig. 9 illustrates the variation of UBHC emission for neat diesel, diesel- *Dunaliella salina* biodiesel and its nano-particle fuel blend at varied compression ratio. Neat diesel exhibited 25 ppm, 31 ppm and 45 ppm of UBHC emission at low, part and full load condition during the CR17.5. Increment and decrement of CR (upto 17 and 18 respectively) when the engine is fueled with diesel and biodiesel blends significantly reduced the UBHC formation at low and part load, but full load condition showcased marginally higher UBHC emission which may be due to the richer air-fuel mixture with shorter time for combustion process. D80DuBD20 fuel blend infused with TiO_2 showcased relatively higher UBHC at CR18. D80DuBD20-$TiO_2$50 at CR18 exhibited 27.61 ppm, 33.35 ppm and 63.25 ppm of UBHC emission whereas D80DuBD20$TiO_2$150 at CR18 exhibited 22.1 ppm, 44.43 ppm and 64.82 ppm of UBHC emission at low, part and full loading condition respectively. 100 ppm of nano particle blended diesel-biodiesel blend showcased marginally lower UBHC of 21.42 ppm, 41.99 ppm and 60.42 ppm across all loading conditions. This may be due to

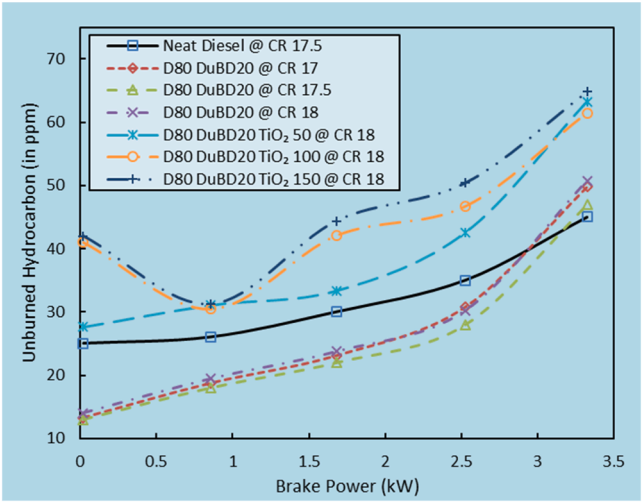

Fig. 9. Variation in Unburned Hydrocarbon at Compression Ratio 17, 17.5 and 18.

better mixing of fuel and air in prominent proportions with enhanced swirl motion inside the combustion chamber at higher compression ratio. Prevention of nano- agglomeration with homogeneous distribution of TiO_2 during the combustion process may also be a reason for reduced UBHC emission. The developed ANN model exhibited higher UBHC emission of 61.20 ppm for D80DuBD20$TiO_2$100 at CR18 under full load condition. Reduction in the TiO_2 concentration upto 50 ppm considerably brought down the UBHC emission upto 42.30 ppm significantly which was very similar to the experimental values [16].

4.4. Carbon monoxide emission

Carbon monoxide emission formation takes place mainly due to incomplete combustion during the premixed combustion phase during the combustion phenomenon. The variation in the CO formation with respect to brake power across the various fuel blends at CR17, 17.5 and 18 are shown in Fig. 10. It can be seen at low loads, neat diesel exhibited 0.028 kg/kWhr of CO emission whereas D80DuBD20 showcased 0.044 kg/kWhr of CO emission. With the increase in engine load, CO emission was gradually escalated upto 0.11 % and 0.125 kg/kWhr for neat diesel and D80DuBD20 at factory set compression ratio. With the decrement in CR (CR17) for D80DuBD20, CO emission was found to be 0.14 % at full load (i.e.) 10.71 % increase in CO emission experimentally and escalated upto 0.126 kg/kWhr in the predicted model. D80DuBD20 at CR18 showcased a CO emission of 0.13 kg/kWhr which is 7.69 % lower than CO emission at CR17 which may be due to improvised combustion process with relatively higher in-cylinder temperature. Addition of TiO_2 with D80DuBD20 at optimal CR18 showcased a marginally escalation in CO emission upto 0.24 kg/kWhr for 50 ppm and 0.26 kg/kWhr for 150 ppm of nano particle infusion. D80DuBD20$TiO_2$100 experimentally exhibited 0.28 kg/kWhr of CO emission at full load condition and 0.05 % at part load operations whereas ANN prediction model exhibited 0.044 kg/kWhr and 0.274 kg/kWhr respectively. TiO_2 dispersion stability during the premixed combustion phase may also be a reason for lower CO emission at part load operations [17,18].

4.5. Carbon di-oxide emission (CO_2)

Fig. 11 depicts the emission of CO_2 of neat diesel, D80DuBD20 and its nano-TiO_2 blends at CR17, 17.5 and 18 during low, part and full load operations. Neat diesel exhibited 3.46 %, 5.09 % and 8.85 % of CO_2 emission on low, part and full load conditions at CR17.5 whereas D80DuBD20 showcased 3.62 %, 5.37 % and 9.17 % of CO_2 emission. The increase in CO_2 emission for diesel-biodiesel blends witnessed better combustion and availability of oxygen atom for the oxidation reaction to take place. Decrement in the CR upto 17 marginally reduced the CO_2 emission by upto 4.5 % to 6 % at higher loading condition, but an increment in the CR upto CR18 significantly increased the CO_2 formation at part load and full load condition by upto 5.21 % and 8.92 % respectively making it more suitable for operation. Further, addition of TiO_2 to D80DuBD20 at CR18 in 50 ppm, 100 ppm and 150 ppm increased the formation of CO2 favoring complete combustion and oxidizing the available CO to CO_2 [42]. D80DuBD20$TiO_2$100 exhibited 3.64 %, 7.01 % and 9.23 % of CO_2 emission at low, part and full load conditions respectively and the outcomes were similar to the data predicted through ANN model. Higher CO_2 emission was forecasted for D80DuBD20@CR18 as 9.058 % during the full load operation.

4.6. Oxides of nitrogen (NO_x)

The emission pattern of NO_x when DuBD20 blends infused with TiO_2 at 50 ppm, 100 ppm and 150 ppm is shown in Fig. 12 at compression ratio of 17, 17.5 and 18. The developed ANN regression model also forecasted similar outcomes as that of the experimental data. The variation of test fuel was compared with neat diesel to understand the engine's behaviour. Generally, nitrogenous oxides are emitted during the combustion process due to the predominant high temperature reaction during the premixed combustion phase of the combustion process. In the

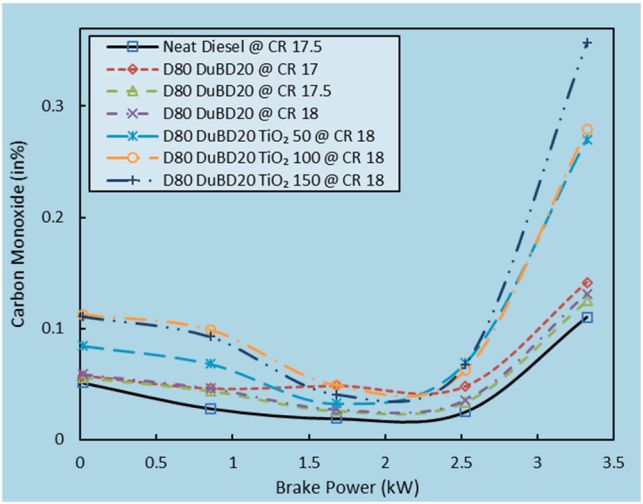

Fig. 10. Variation in Carbon monoxide at Compression Ratio 17, 17.5 and 18.

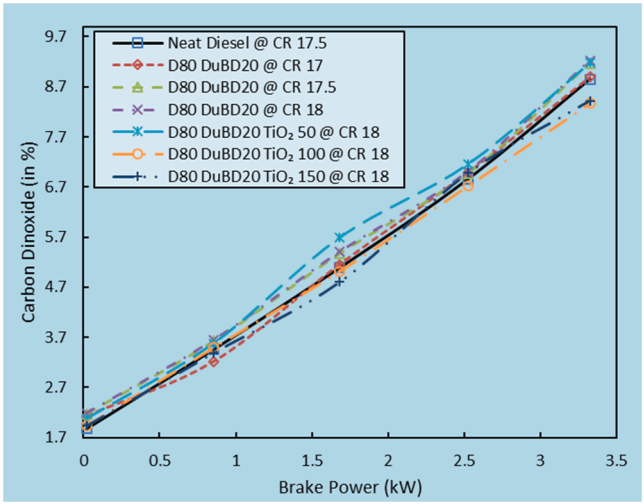

Fig. 11. Variation in Carbon dioxide at Compression Ratio 17, 17.5 and 18.

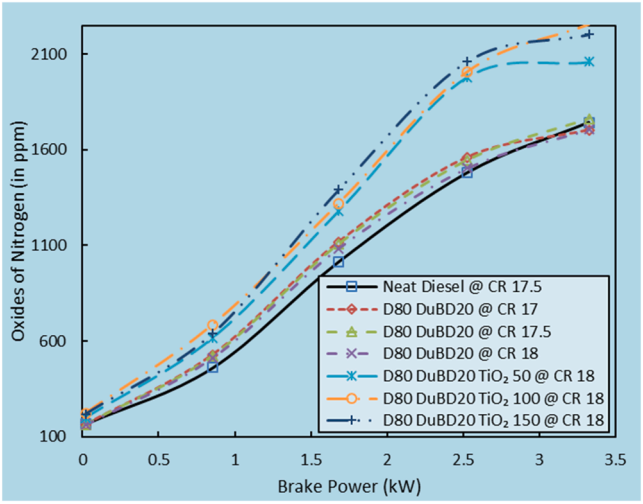

Fig. 12. Variation in Oxides of Nitrogen at Compression Ratio 17, 17.5 and 18.

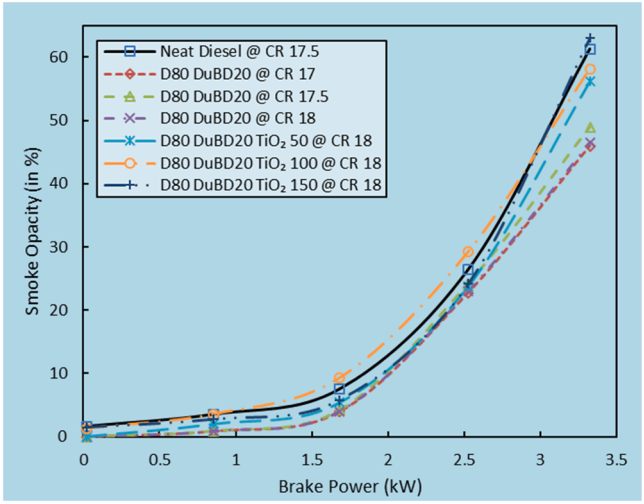

Fig. 13. Variation in Smoke opacity at Compression Ratio 17, 17.5 and 18.

present investigation, TiO_2 nano-particle releases additional oxygen due to micro-explosion which make the combustion process enriched thereby the combustion duration and the peak in-cylinder temperature escalates enormously generating higher quantity of mono-atomic nitrogen and oxygen atom as stated in the Zeldovich mechanism, especially at CR18. At factory set compression ratio (CR 17.5) and decremented compression ratio (CR17), the NO_x emission was significantly reduced due to decreased total heat capacity of the gaseous mixture inside the combustion chamber specifically around the cervices volume. Reduction in engine NO_x was mainly due to increase in working gases total heat capacity consequently affecting the peak in-cylinder temperature. Reduction in engine NO_x can be alternatively witnessed with reduced engine power and thermal efficiency with relatively higher fuel consumption especially at low and part load operation [43]. From the Fig. 12, it could be observed that neat diesel exhibited 460 ppm of NO_x at low load in CR17.5. D80DuBD20 test fuel, at the same CR of 17.5, emitted 527 ppm of NO_x which was 1.27 % higher. Amalgamation of TiO_2 with diesel-biodiesel blend further increased the emission of NO_x by upto 686 ppm (experimentally) and 683.13 ppm (ANN Prediction) at low load. It can also be noted that the decrement in CR upto 17 marginally reduced the NO_x emission by 0.12 %. With variation in TiO_2 concentration by 50 ppm, 100 ppm and 150 ppm with D80DuBD20 test fuel, the NO_x emission was 1280 ppm, 1320 ppm, 1390 ppm at part load and 2060 ppm, 2254 ppm, 2204 ppm at full load operations. ANN model showcased the NO_x emission of 1978.54 ppm, 2252.26 ppm and 2059.95 ppm at full load condition. It can be seen that, infusion of TiO_2 with D80DuBD20 upto 100 ppm significantly escalated the NO_x emission which could be overcome by incorporating suitable after-treatment techniques like Selective Catalytic Reduction, Exhaust Gas Recirculation and Lean NO_x trap methods.

4.7. Smoke opacity

The higher composition of carbon atom in the fuel and its oxidation capability determines the formation of smoke in compression ignition engine. Fig. 13 shows the variation in smoke opacity with various test fuel blends at CR 17, 17.5 and 18. It can be clearly noticed that neat diesel produced higher amount of smoke at all load condition due to the splintering of carbon atom and less time availability for the oxidation reaction to take place. Smoke emission was lessened with D80DuBD20 fuel at CR17 due to availability of surplus oxygen atom and be better atomization. Increase in the CR upto 18 with diesel-biodiesel blend also had a negligible effect on the smoke formation. Amalgamating 50 ppm of TiO2 with D80DuBD20 showed significant elevation of smoke emission by upto 5.45 % at part load and 55.45 % at full load condition when the engine was operating at CR18. Increment in TiO_2 upto 100 ppm and 150 ppm further increased the smoke formation marginally by upto 2.323 %. This may be due to relatively higher viscosity of the fuel, lesser availability of O_2 at high compression ratio, poor atomization and increased number of fuel rich zone in the combustion chamber. This could be overcome by injecting the fuel at higher pressure thereby enhanced atomization of the fuel droplet takes place and adopting after treatment techniques like EGR and SCR [27,38].

The variation in the performance and emission phenomenon across all test fuel blends at CR 17, 17.5 and 18 are showcased in Fig. 14. A comparative table detailing the performance and emission phenomenon of CI engine fuelled with *Dunaliella salina* – diesel blends amalgamated with TiO_2 with other micro-macro algal biodiesel is presented in Table 11. The insights of variation in BTE, BSFC, HC, CO, NO_x and smoke emission are tabulated for better understanding.

5. ANN prediction

Table 9 and 10 depicts the variation of outcomes between the ANN Predicted data and experimental data at all compression ratio (17, 17.5 and 18) for diesel, diesel-Dunillia salina biodiesel blends with infusion of TiO_2 at 50, 100 and 150 ppm. The input parameters for the developed ANN model are the test fuel blend (diesel (D100), Diesel-Dunillia salina biodiesel blend (D80DuBD20), Diesel-Biodiesel-Nano particle blend (D80DuBD20$TiO_2$50, 100 and 150 ppm) with variation in compression ratio (17, 17.5 and 18), test fuel properties (density, flash and fire point, calorific value and kinematic viscosity), engine speed and load, instantaneous fuel consumption, intake manifold temperature / pressure and relative humidity. The output parameters are BTE, BSFC, CO, UBHC, CO_2, NO_x, Smoke and RMS values. The effect of individual parameters on the emission and performance characteristics were evaluated using ANN regression model developed variable ANN structuring iterations to obtain the optimal output which was in-line with the experimental outcomes under numerous evaluation criteria. The training algorithm in the present assessment was developed considering a combination of log-sig and tan-sig function using one hidden layer and the output layer selection was carried out using the purelin transfer function of 25 neurons. The R value (correlation co-efficient) was identified as 0.998, 0.993 and 0.996 for training, validation and testing algorithm of the optimal outcomes. The Mean Square Error (MSE) for training, validation and testing was noted as 0, 22.56, 58.99 respectively. In order to assess the network response, the corresponding target along with the network output were analyzed in the present regression analysis. The regression co-efficient for BTE, BSFC, CO, UBHC, CO_2, NO_X and smoke were identified as 0.96, 0.98, 0.97, 0.99, 0.96, 0.94 and 0.98 respectively. The

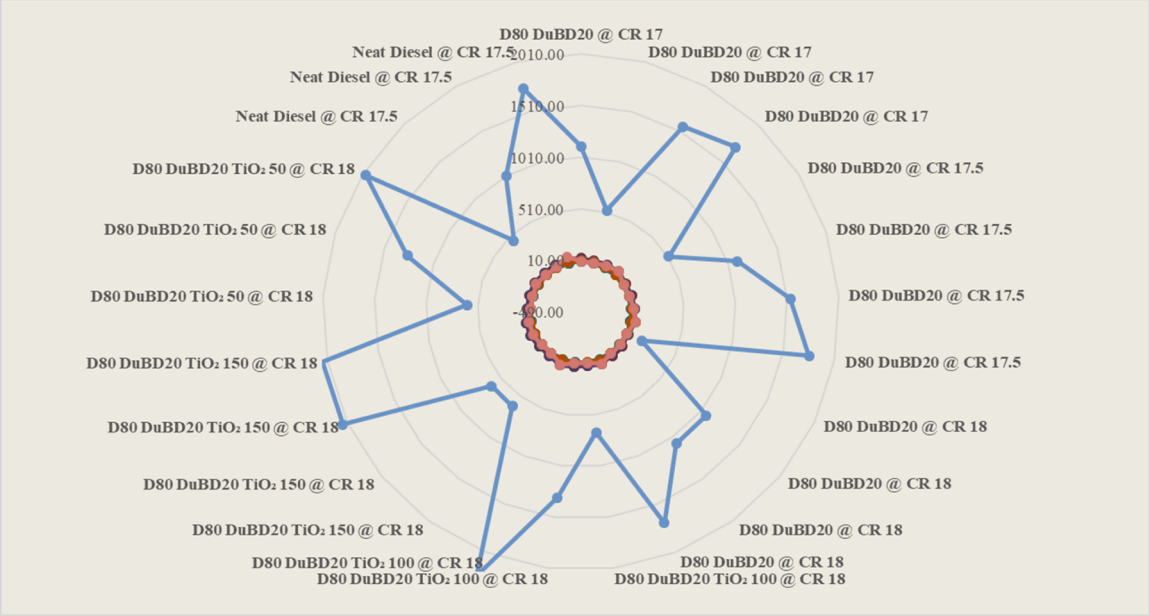

Fig. 14. Comparison of test fuel behaviour on engine's performance and emission phenomenon in a Radar plot at CR 17, 17.5 and 18.

Table 9
Experimental outcomes of performance and emission.

Run	Load	Fuel Type	Experimental data						
			BTE	**BSFC**	**UBHC**	**CO**	**CO_2**	**NO_x**	**Smoke**
11	25	Neat Diesel @ CR 17.5	22.69	3.24	26.00	0.03	3.46	460	3.50
10	50	Neat Diesel @ CR 17.5	31.77	0.28	30.00	0.02	5.09	1015	7.50
4	100	Neat Diesel @ CR 17.5	35.87	0.24	45.00	0.11	8.85	1744	61.30
16	25	D80 DuBD20 @ CR 17	22.24	3.49	18.72	0.05	3.21	527	0.85
23	50	D80 DuBD20 @ CR 17	31.13	0.29	23.10	0.05	5.16	1118	3.95
6	100	D80 DuBD20 @ CR 17	35.15	0.26	49.82	0.14	8.89	1703	45.97
9	25	D80 DuBD20 @ CR 17.5	20.02	3.42	18.00	0.04	3.62	522	0.90
25	50	D80 DuBD20 @ CR 17.5	29.88	0.28	22.00	0.03	5.37	1107	4.20
7	100	D80 DuBD20 @ CR 17.5	33.22	0.25	47.00	0.13	9.17	1762	48.90
2	25	D80 DuBD20 @ CR 18	30.98	0.31	23.76	0.03	5.40	1085	3.99
14	50	D80 DuBD20 @ CR 18	30.98	0.31	23.76	0.03	5.40	1085	3.99
12	100	D80 DuBD20 @ CR 18	32.48	0.28	50.76	0.13	9.23	1707	46.46
21	25	D80 DuBD20 TiO_2 50 @ CR 18	22.96	3.84	31.05	0.07	3.58	616	1.98
18	50	D80 DuBD20 TiO_2 50 @ CR 18	33.41	0.36	33.35	0.03	5.69	1280	5.38
15	100	D80 DuBD20 TiO_2 50 @ CR 18	36.55	0.30	42.55	0.07	7.16	1981	23.74
3	25	D80 DuBD20 TiO_2 100 @ CR 18	29.18	3.89	30.50	0.10	3.49	686	3.56
19	50	D80 DuBD20 TiO_2 100 @ CR 18	40.79	0.37	42.10	0.05	5.02	1320	9.27
20	100	D80 DuBD20 TiO_2 100 @ CR 18	46.60	0.28	61.45	0.28	8.37	2254	58.15
5	25	D80 DuBD20 TiO_2 150 @ CR 18	27.34	3.98	31.20	0.09	3.39	638	2.73
17	50	D80 DuBD20 TiO_2 150 @ CR 18	27.88	4.06	31.82	0.09	3.45	651	2.78
24	100	D80 DuBD20 TiO_2 150 @ CR 18	43.25	0.26	50.40	0.07	6.98	2062	24.12

experimental outcomes and ANN predictions are tabulated in Table 9 which explicitly shows the developed ANN model closely predicts the performance and emission phenomenon of the CI engine and proved itself satisfactory with a limited number of data's which drastically reduced the engine's calibration cost and data collection/calculation time period.

6. Relative impact of the input parameters

The input factor contributions on the output parameters in the developed ANN model with 10 hidden neurons is described in Fig. 15. It can be observed that the biodiesel blends and load have a positive vital effect on the output parameters. RI of biodiesel blends and load are 61 % and 45 %. However, biodiesel blends have comparatively small difference of 16 % to load. This implies that both biodiesel blends and load are significant factors in the modeling performance and emission of engine fueled with biodiesel, biodiesel blends contribute more influence [22].

7. Techno-economic analysis

The *Dunaliella salina* biodiesel production plant design has a capacity of 120 thousand tons per year in 335 working days. The entire plant was erected in June 2024 and has an estimated life time of 25 years. The cost of *Dunaliella salina* biodiesel plant was divided into two main categories, namely capital investment expenditure and operating variable expenditure as shown in the Fig. 16.

7.1. Capital investment expenditure (CAIEXP)

Capital Investment Expenditure is a one-time investment needed to procure and establish the bio-oil and its biodiesel production cost during the start of the project plant. It is categorized as Fixed equipment cost,

Table 10
ANN predictive outcomes of performance and emission.

Run	Load	Fuel Type	ANN Predicted data						
			BTE	**BSFC**	**UBHC**	**CO**	**CO_2**	**NO_x**	**Smoke**
11	25	Neat Diesel @ CR 17.5	22.54	3.14	25.75	0.023	3.28	458.01	3.42
10	50	Neat Diesel @ CR 17.5	31.61	0.18	29.75	0.014	4.91	1013.01	7.42
4	100	Neat Diesel @ CR 17.5	35.72	0.14	44.75	0.105	8.67	1742.01	61.22
16	25	D80 DuBD20 @ CR 17	22.09	3.39	18.47	0.041	3.03	525.23	0.77
23	50	D80 DuBD20 @ CR 17	30.98	0.18	22.85	0.044	4.98	1116.08	3.87
6	100	D80 DuBD20 @ CR 17	35.00	0.15	49.57	0.136	8.72	1700.63	45.89
9	25	D80 DuBD20 @ CR 17.5	19.87	3.32	17.75	0.039	3.44	520.01	0.82
25	50	D80 DuBD20 @ CR 17.5	29.73	0.18	21.75	0.021	5.19	1105.01	4.12
7	100	D80 DuBD20 @ CR 17.5	33.07	0.15	46.75	0.120	8.99	1760.01	48.82
2	25	D80 DuBD20 @ CR 18	30.83	0.21	23.51	0.022	5.22	1082.87	3.91
14	50	D80 DuBD20 @ CR 18	30.83	0.21	23.51	0.022	5.22	1082.87	3.91
12	100	D80 DuBD20 @ CR 18	32.33	0.18	50.51	0.126	9.05	1704.77	46.38
21	25	D80 DuBD20 TiO_2 50 @ CR 18	22.81	3.74	30.80	0.063	3.40	613.90	1.90
18	50	D80 DuBD20 TiO_2 50 @ CR 18	33.26	0.26	33.10	0.028	5.51	1278.25	5.30
15	100	D80 DuBD20 TiO_2 50 @ CR 18	36.40	0.20	42.30	0.064	6.98	1978.54	23.66
3	25	D80 DuBD20 TiO_2 100 @ CR 18	29.03	3.78	30.25	0.094	3.31	683.81	3.48
19	50	D80 DuBD20 TiO_2 100 @ CR 18	40.64	0.27	41.85	0.044	4.84	1318.19	9.19
20	100	D80 DuBD20 TiO_2 100 @ CR 18	46.45	0.18	61.20	0.274	8.19	2252.26	58.07
5	25	D80 DuBD20 TiO_2 150 @ CR 18	27.19	3.88	30.95	0.088	3.21	635.98	2.65
17	50	D80 DuBD20 TiO_2 150 @ CR 18	27.73	3.96	31.57	0.089	3.27	648.70	2.70
24	100	D80 DuBD20 TiO_2 150 @ CR 18	43.10	0.16	50.15	0.062	6.80	2059.95	24.04

Table 11
Comparison of the performance and emission phenomenon of *Dunaliella salina* microalgae with other feedstock's in compression ignition engines.

Engine type	Fuel blend	Oxygenated additive	Emission parameters	Performance parameters	References
1 Cylinder, 1500 rpm 3.5 kW 220 bar	*Dunaliella salina* biodiesel with diesel	TiO_2 nanoparticle at 50, 100 and 150 ppm at varied CR	HC ↑ by 2.43 %, CO ↑ by 3.01 %, NOx ↑ by 3.47 % and smoke ↓ by 1.42 % at CR 18 with TiO_2 100 ppm	BTE ↑ by 6.45 %, BSFC ↓ by 3.57 % at CR 18 with TiO_2 100 ppm	Present study
4 stroke, 3.5 kW 1500 rpm CI engine	*Chlorella vulgaris* biodiesel with diesel	Ammonium hydroxide (5 % and 10 % volumetric blend)	HC ↓ by 16.82 %, CO ↓ by 14.15 % and smoke ↓ by 8.23 % with EGR	BTE ↑ by 1.92 %, BSFC ↓ by 9.54 % with EGR	Vellaiyan [4]
Vertical 4S DI, 3.7 kW, 1500 rpm CI engine	Spirulina microalgal biodiesel with diesel	–	HC ↓ by 12.10 %, NO_x ↑ by 2.42 %, CO ↓ by 0.25 %	BTE ↑ by 1.78 %, BSFC ↓ by 12.78 % and $\prod_{vol}$ ↓ by 0.32 %`	Alzubaidi et al. [26]
1C, 4S, All06A2 swirl combustion chamber, 11 kW, 2200 rpm CI engine	*Scenedesmus obliqus* algal biodiesel with diesel	n-pentane at 5 %, 10 % and 15 % blend ratio	NO_x ↓ by 35.4 %, HC ↓ by 7.23 % and CO_2 ↑ by 21.3 %	BTE ↑ by 7.12 % and BSFC ↓ by 6.24 %	Sekar et al. [15]
Kirloskar 1C, 4S 8.5 kW, 3000 rpm CI engine	*Scenedesmus dimorphous* microalgal biodiesel with diesel	H_2 gas supplemtation at 5 LPM	NO_x ↑ by 21.78 %, CO ↓ by 35.54 % and CO_2 ↓ by 12.02 %	BP ↑ by 4.32 % and BSFC ↓ by 11.47 %	Rashd et al. [6]
1C, 3.5 kW, 1500 rpm CI engine	Spirogyra algal biodiesel with diesel	H_2 gas at 5, 10 and 15 LPM with Di-terbutyl peroxide at 3.3 %	HC ↓ by 38.8 %, CO ↓ by 64.8 %, smoke ↓ by 29.21 % and NO_x ↓ by 32.6 %	BSFC ↓ by 36.2 % and BTE ↑ by 36.2 %	Adib et al. [5]
Hazt 1 B 30–2 model, 1C, 4S Aircooled CI engine	*C. cohnii* microalgae biodiesel with diesel	CeO_3 and Fe_2O_3 nanoparticle	NO_x ↑ by 8.37 %, PM ↓ by 1.34 % and smoke ↓ by 2.32 %	BSFC ↑ by 2.58 % and BTE ↑ by 5.67 %	Stevenson et al. [42]

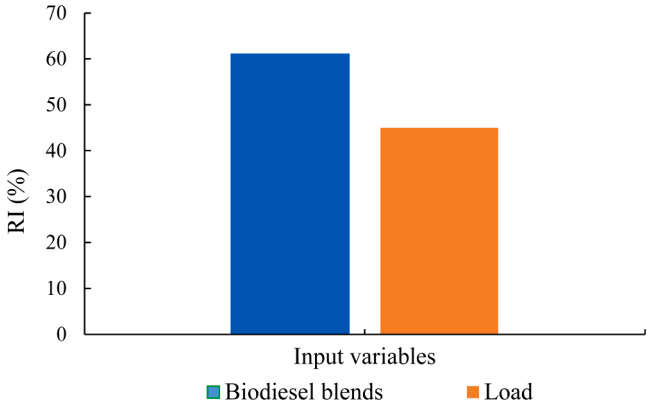

Fig. 15. RI of biodiesel blends and load used in the developed ANN model.

cost of installation and other associated expenses. These expenses are related to purchase and installation of equipment involved in the production of bio-oil and its biodiesel. The equipment installation cost also caters the plumbing, electrical, piping, instrumentation and other related activities. The total CAIEXP classified under fixed equipment cost (FEC) and cost of installation and other associated expenses (C_iOEXP) in USD are tabulated in Table 12 with comparison from the literature [44].

7.2. Operating variable expenditure (OPVEXP)

Operating Variable Expenditure encompasses the expenses involved periodically in running the *Dunaliella salina* biodiesel plant. This is further classified as Fixed and variable expenses. The Fixed expenses are those which are to be paid on the yearly basis like insurance, calibration and maintenance even if the biodiesel plant is in non-operational condition. The variable expenses are those non-fixed expenses which are being paid when the biodiesel plant is in operation condition like algal feed stock, bio reactor, nutrients, carbon di-oxide and nitrogen gas, chemical solvents – reagents and other utilities [46]. The expenses involved in producing the feedstock like cultivation, nutrient solution, harvesting, drying and pelletization process are also summarized. Direct skilled technicians and labors are estimated to be 50 employees which

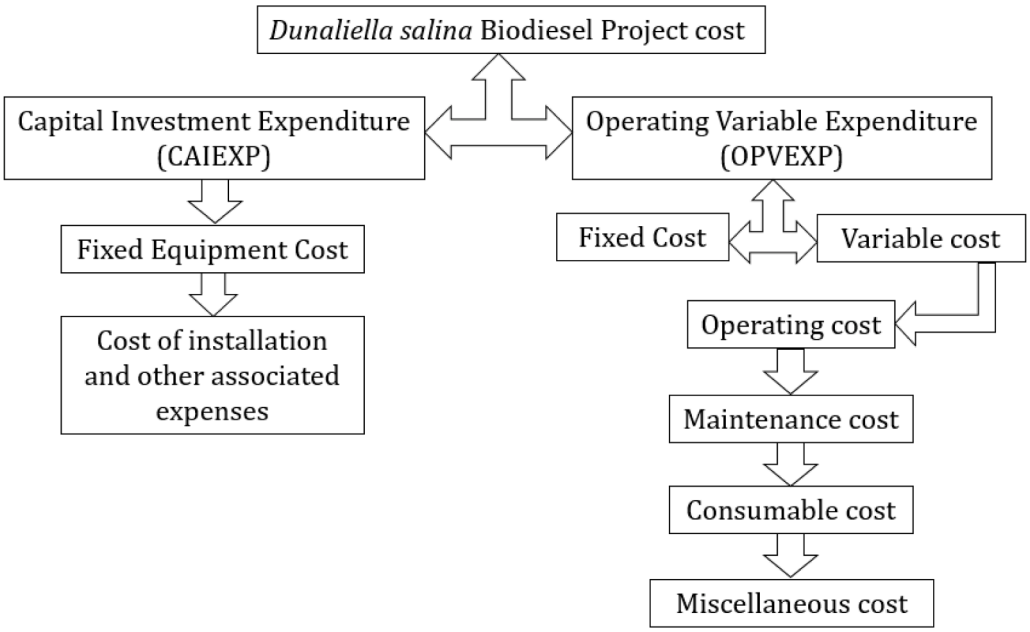

Fig. 16. Capital Investment Expenditure (CAIEXP) and Operating Variable Expenditure (OPVEXP).

Table 12
Project indicator for *Dunaliella salina* biodiesel plant.

Techniques	FEC	CiOEXP	Total CAIEXP	Ref.
Single stage transesterification	78,500	45,200	123,700	Present study
Ultrasonic assisted transesterification	87,250	71,450	158,700	Abdallah et al. [44]
Microwave assisted transesterification	67,320	40,150	107,470	Naveenkumar et al. [45]

include technical personnel, engineers, accountants, HR personnel etc. and their average salary will be around 375 USD per month per employee. Therefore, the annual expenditure toward salary head will be around 13,420 USD. The expected skilled technician and labor cost until 2049 with an annual inflation of 3.5 % would be around 3,35,500 USD. Inflations are expected to be in rise constantly with time period. The annual inflation for skilled labor was considered as 3.5 % whereas for OPVEXP, is was set as 1.8 %.

7.3. Biodiesel project indicators (BPI)

The revenue of the project is indicated by multiplying the cost of *Dunaliella salina* biodiesel per ton with the total production of *Dunaliella salina* biodiesel. It is also the inclusive cost growth culture, photo-bioreactor, cultivation, harvesting and pelletization technique of the feedstock. The cost of *Dunaliella salina* biodiesel was 1650 USD per ton with an annual inflation of 1.8 %.

Net income and Gross profit are the two critical indicator which showcases the feasibility and successfulness of the biodiesel project. Gross profit (GP) is termed as the deduction of operating variable expenditure (OPVEXP) from the revenue of the project (P_r) as shown in Eq. (13).

$$Gross\ Profit\ (GP) = Revenue\ of\ the\ project\ (P_r) - Operating\ Variable\ Expenditure\ (OPVEXP) \quad (13)$$

Net Income is termed as the remains of money after the deduction of depreciation cost, insurance, taxes etc. from the Gross Profit (GP). The bottom line of the income statement generally notifies the Net Income (N_i) and can be expressed as in Eq. (14).

$$Net\ Income\ (N_i) = Gross\ Profit\ (GP) - (Depreciation + Insurance + Taxes) \quad (14)$$

The sheet of Income Statement is a tabulation used to assess the financial status of the biodiesel project and it includes the major financial indicators like Gross Profit, revenue, expenses, net profit and loss with taxation at 18 % GST on the Gross profit.

Single stage transesterification using ANN predicted multiple combinations of molar ratio, catalyst concentration and reaction time. A fluctuation in the yield of *Dunaliella salina* biodiesel can be noticed in Table 1. The optimal combination showcased was 1:8 molar ratio, 0.75 % by weight of NaOH, 85 °C reaction temperature and 110 min of reaction duration across all condition yielded 91.2 % of *Dunaliella salina* biodiesel experimentally. To sum up, the above combination also achieved a superior net profit on comparison with other combinations which was because of higher transesterification efficacy with lower quantity of NaOH and methanol. Fig. 17 compares the biodiesel production cost of 1 L by single stage transesterification method with ultrasonic and microwave assisted esterification process and proved to be lower than other techniques globally [45].

The difference between present money value of cash outflow and

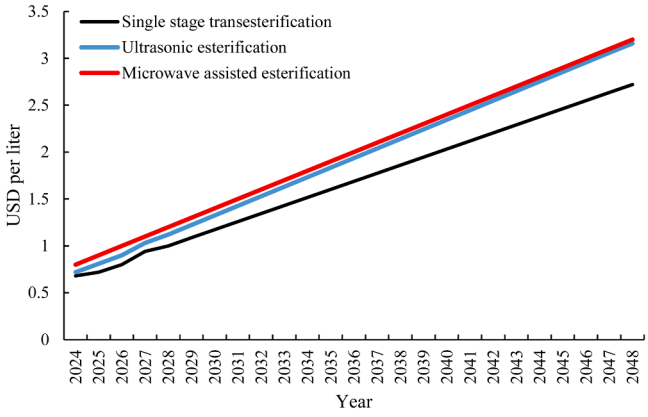

Fig. 17. Predicted cost of Dunaliella salina biodiesel production in the project period.

present money value of cash inflow determines the Net Present Value (NPV). Is the NPV is positive, then it indicates that the biodiesel project is a feasible and profitable one thereby the expenses are lower than the earnings. Table 13 compares the NPV of single stage transesterification process with other techniques reported in literature and found to be profitable [44,45].

Decision making in selecting the best economic methodology in deriving the *Dunaliella salina* biodiesel based in the cost benefit analysis is termed as Profitability Index (PI). It is the ratio between Net Present value and Initial Capital Expenditure as shown in Equation 15

$$PI = \frac{NPV}{Initial\ Capital\ Expenditure} \tag{15}$$

Profitability index of the selected single stage transesterification process was found to be 8.67 whereas literature reported PI for ultrasonic and microwave assisted transesterification are 6.73 and 7.92 respectively.

The ratio illustrating the Net Profit and Net overall cost during the entire period is termed as Return on Investment (ROI) and is also the measure of profitability. Eq. (16) was used to measure the ROI and Table 13 shows the ROI of the present investigation comparing the other methods from the literature.

$$ROI = \left(\frac{Total\ revenue - Cost\ of\ the\ project}{Total\ project\ cost}\right) = \frac{Net\ Profit}{Total\ Project\ Cost} \tag{16}$$

7.4. Economic performance

The economic performance indicators like NPV, PI, ROI, GP, N_i and P_r were analyzed in this section. *Dunaliella salina* biodiesel is the main product which is related to the revenue stream and its cost per liter is predicted to be varying between 0.72 USD and 3.12 USD across the plant life. The total capital investment expenditure is 123,700 USD as shown in Table 12. It is to be also noted that NaOH and methanol recovery add 41,105 USD per year. The recovery solvent and catalyst is purified and used for the subsequent batch cycle of transesterification reaction thereby significant reduction in the operation cost was witnessed. As discussed, the biodiesel plant has a life time of 25 years with a payback period of 1 year and 7 months and the NPV of single stage transesterification process is 472,414 USD at 10 %.

8. Conclusion

This study comprehensively investigated the effects of TiO_2 nanoparticle additives at varying compression ratios in a CI engine fueled with *Dunaliella salina* biodiesel-diesel blends. Additionally, an Artificial Neural Network (ANN) model was developed to predict engine performance and emission characteristics, and its outcomes were validated against experimental results.

Key findings of the study are summarized as follows:

- *Dunaliella salina* was successfully cultivated in an aseptic laboratory environment using an f/2 nutrient medium under nitrogen-deficient conditions yielding 675 ml of algal oil.
- A single-stage transesterification process using NaOH and methanol (1:8 molar ratio, 0.75 % catalyst by weight, 75 °C reaction temperature, and 110-minute reaction duration) resulted in a 91.2 % transesterification efficiency and was confirmed by the ANN approach, producing 485 ml of biodiesel.
- Spectroscopic analysis confirmed the successful conversion of algal oil into biodiesel. FTIR spectra indicated the transformation of long-chain hydrocarbons into fatty acid methyl esters (FAMEs) with Linolenic acid and Arachidic acid as dominant compounds.
- The ANN model, developed using the Levenberg-Marquardt algorithm with 27 datasets, effectively predicted engine performance and emission characteristics for different compression ratios (CR17, CR17.5, and CR18).
- At CR18, the D80DuBD20TiO_{2100} blend exhibited the highest brake thermal efficiency (BTE) of 46.45 % at full load, closely matching the ANN-predicted value of 46.6 %.
- TiO_2 addition up to 50 ppm increased brake-specific fuel consumption (BSFC) by 6.044 %, while a further increase to 100 ppm led to reduced BSFC values of 18.11 kg/kWhr, 0.36 kg/kWhr, and 0.30 kg/kWhr for low, part, and full load conditions, respectively.
- The lowest unburned hydrocarbon (UBHC) emissions (42.30 ppm at full load) were observed for the D80DuBD20$TiO_2$50 blend, as forecasted by the ANN model.
- Carbon monoxide (CO) emissions were minimized at CR18 for the D80DuBD20 blend, reaching 0.13 kg/kWhr—a 7.69 % reduction compared to CR17.
- NO_x emissions increased significantly at CR18 with the addition of TiO_2, while lower compression ratios (CR17 and CR17.5) exhibited comparatively reduced NO_x levels.
- The ANN model demonstrated strong predictive capability, with correlation coefficients (R) of 0.998, 0.993, and 0.996 for training, validation, and testing, respectively.
- The techno-economic analysis on the production of Dunaliella salina biodiesel was demonstrated the NPV of 472,414 USD with a payback period of 1 year and 7 months.

Overall, the findings of this study highlight the potential of *Dunaliella salina* biodiesel as a sustainable fuel alternative in CI engines, particularly when optimized with TiO_2 nanoparticle additives. The ANN model proved to be a reliable predictive tool for assessing engine performance and emissions, offering a valuable approach for optimizing biodiesel utilization. Future research focuses on the implementation of Selective Catalytic Reduction (SCR) and Particulate traps can considerably reduce the CO, HC NO_x and Smoke emission. Also, a modification in the combustion chamber geometry with swirl combustion chamber will enhance the atomization of fuel particles greatly thereby better BTE can be achieved with reduced BSFC.

Table 13
Project indicator for *Dunaliella salina* biodiesel plant.

Techniques	NPV ($)	PI	ROI (%)	Ref.
Single stage transesterification	472,414	8.67	27.12	Present study
Ultrasonic assisted transesterification	842,103	6.73	20.43	Abdallah et al. [44]
Microwave assisted transesterification	935,613	7.92	19.32	Naveenkumar et al. [45]

Declaration of generative AI in scientific writing

The authors acknowledge the use of AI-assisted tools, notably Grammarly, to improve linguistic accuracy, correct grammatical errors, and increase the overall coherence of this article. The content, analytical discussion, and conclusions presented in this work are distinctly the original contributions of the author, with AI tools utilized solely to enhance the presentation and clarity of the text. The use of AI complies with the journal's requirements for transparency and ethical norms in authorship processes.

CRediT authorship contribution statement

V Hariram: Data curation, Conceptualization. **S Balamurugan:** Methodology, Investigation. **R Mohan:** Software, Resources. **R Karthick:** Funding acquisition, Formal analysis. **Nandagopal Kaliappan:** Investigation. **K Barathiraja:** Validation. **J Godwin John:** Funding acquisition, Formal analysis. **K Kamakshi Priya:** Software, Resources.

Declaration of competing interest

The authors declare that they have no known competing financial interests or personal relationships that could have appeared to influence the work reported in this paper.

Data availability

No data was used for the research described in the article.

References

[1] P. Appavu, Effect of injection timing on performance and emission characteristics of palm biodiesel and diesel blends, J. Oil Palm Res. 30 (2018) 674–681, https://doi.org/10.21894/jopr.2018.0057.

[2] S.O. Bitire, T.C. Jen, An optimization study on a biosynthesized nano-particle and its effect on the performance-emission characteristics of a diesel engine fueled with parsley biodiesel blend, Energy Rep. 9 (2023) 2185–2200.

[3] H. Venu, L. Subramani, V.D. Raju, Emission reduction in a DI diesel engine using exhaust gas recirculation (EGR) of palm biodiesel blended with TiO2 nano additives, Renew. Energy 140 (2019) 245–263.

[4] S. Vellaiyan, Optimizing algae biodiesel blends with aqueous ammonia and nanocomposite for enhanced performance and environmental benefits, Case Stud. Chem. Environ. Eng. 9 (2024) 100698.

[5] A.R. Adib, M.M. Rahman, T. Hassan, M. Ahmed, A. Al Rifat, Novel biofuel blends for diesel engines: optimizing engine performance and emissions with C. cohnii microalgae biodiesel and algae-derived renewable diesel blends, Energy Convers. Manag.: X 23 (2024) 100688.

[6] D. Yuvarajan, M. Venkata Ramanan, Investigation on effect of magnetite nanofluid on performance and emission patterns of methyl esters of bio diesel, J. Environ. Eng. Landsc. Manag. 24 (2) (2016) 90–96, https://doi.org/10.3846/16486897.2016.1142447.

[7] S.S. Kattimani, S.N. Topannavar, M.M. Shivashimpi, B.M. Dodamani, Experimental investigation to optimize fuel injection strategies and compression ratio on single cylinder DI diesel engine operated with FOME biodiesel, in: Energy, 200, 2020 117336.

[8] G.P. Rao, L.S.V. Prasad, Combined influence of compression ratio and exhaust gas recirculation on the diverse characteristics of the diesel engine fueled with novel palmyra biodiesel blend, Energy Convers. Manag.: X 14 (2022) 100185.

[9] M. Santhosh, K.P. Padmanaban, Experimental investigation on engine performances, combustion characteristics and emission of exhaust gases of VCR engine fuelled with cottonseed oil methyl ester blended with diesel, Int. J. Green. Energy 13 (14) (2016) 1534–1545.

[10] N. Bhanu Teja, Y. Devarajan, R. Mishra, S. Sivasaravanan, D. Thanikaivel Murugan, Detailed analysis on sterculia foetida kernel oil as renewable fuel in compression ignition engine, Biomass Convers. Biorefinery 13 (4) (2021) 2959–2970, https://doi.org/10.1007/s13399-021-01328-w.

[11] S. Patnaik, N. Khatri, E.R. Rene, Artificial neural networks-based performance and emission characteristics prediction of compression ignition engines powered by blends of biodiesel derived from waste cooking oil, Fuel 370 (2024) 131806.

[12] S.H. Hosseini, A. Taghizadeh-Alisaraei, B. Ghobadian, A. Abbaszadeh-Mayvan, Artificial neural network modeling of performance, emission, and vibration of a CI engine using alumina nano-catalyst added to diesel-biodiesel blends, Renew. Energy 149 (2020) 951–961.

[13] S. Javed, Y.S. Murthy, R.U. Baig, D.P. Rao, Development of ANN model for prediction of performance and emission characteristics of hydrogen dual fueled diesel engine with Jatropha Methyl Ester biodiesel blends, J. Nat. Gas. Sci. Eng. 26 (2015) 549–557.

[14] C.P. Okonkwo, V.I.E. Ajiwe, M.C. Obiadi, M.O. Okwu, J.I. Ayogu, Production of biodiesel from the novel non-edible seed of Chrysobalanus icaco using natural heterogeneous catalyst: modeling and prediction using Artificial Neural Network, J. Clean. Prod. 385 (2023) 135631.

[15] M. Sekar, M.Y. Selim, M. Elgendi, Improving the performance of a diesel engine using nanomaterials and chlorella vulgaris microalgae blends assisted with biogas, Int. J. Hydrog. Energy 49 (2024) 496–506.

[16] P. Sivamurugan, Y. Devarajan, Emission analysis of dual fuelled diesel engine, Int. J. Ambient Energy 42 (1) (2018) 15–17, https://doi.org/10.1080/01430750.2018.1517696.

[17] A. Samadi-Koucheksaraee, S. Shirvani-Hosseini, I. Ahmadianfar, B. Gharabaghi, Optimization algorithms surpassing metaphor, eds, in: O. Bozorg-Haddad, B. Zolghadr-Asli (Eds.), Computational Intelligence for Water and Environmental Sciences, Computational Intelligence for Water and Environmental Sciences, 1043, Springer, Singapore, 2022, https://doi.org/10.1007/978-981-19-2519-1_1. Studies in Computational Intelligence.

[18] Y. Fang, I. Ahmadianfar, A. Samadi-Koucheksaraee, R. Azarsa, M. Scholz, Z. M. Yaseen, An accelerated gradient-based optimization development for multi-reservoir hydropower systems optimization, Energy Rep. 7 (2021) 7854–7877, https://doi.org/10.1016/j.egyr.2021.11.010.

[19] A. Naseri, M. Jamei, I. Ahmadianfar, Nanofluids thermal conductivity prediction applying a novel hybrid data-driven model validated using Monte Carlo-based sensitivity analysis, Eng. Comput. 38 (Suppl 1) (2022) 815–839, https://doi.org/10.1007/s00366-020-01163-z.

[20] Manikandan. Sivasubramanian, Vickram. Sundaram, Deena. Santhana Raj, Subbaiya Ramasamy, Karmegam. Natchimuthu, Critical review on fostering sustainable progress: an in-depth evaluation of cleaner production methodologies and pioneering innovations in industrial processes, J. Clean. Prod. 452 (2024) 142207, https://doi.org/10.1016/j.jclepro.2024.142207.

[21] B. Musthafa, M.A. Asokan, Numerical and experimental investigation of performance and emission characteristics of hydrogen enrichment with prosopis juliflora biodiesel in CI engine using RSM and ANN optimization, Int. J. Hydrog. Energy 66 (2024) 326–336.

[22] C.N. Ude, O.D. Onukwuli, N.N. Uchegbu, J.C. Umeuzuegbu, N.F. Amulu, Evaluation of engine performance and emission of African pear seed oil (APO) biodiesel and its prediction via multi-input-multi-output artificial neural network (ANN) and sensitivity analysis, Biofuels Bioprod. Biorefining 15 (3) (2021) 703–718.

[23] N.Ude. Callistus, O.Onukwuli. Dominic, C.Okey-Onyesolu. Faith, C.Nnaji. Patrick, C.Okoye. Chukwunonso, C.Uwaleke. Chidebe, Prediction of some thermo-physical properties of biodiesel using ANFIS and ANN cum sensitivity analysis, Clean. Waste Syst. 2 (2022) 100006.

[24] M. El-Adawy, M. El-Kasaby, Y.A. Eldrainy, Performance characteristics of a supercharged variable compression ratio diesel engine fuelled by biodiesel blends, Alex. Eng. J. 57 (4) (2018) 3473–3482.

[25] D. Yuvarajan, M. Venkata Ramanan, D. Christopher Selvam, Performance analysis on mustard oil methyl ester as a potential alternative fuel, Ind. J. Sci. Technol. 9 (37) (2016), https://doi.org/10.17485/ijst/2016/v9i37/101982.

[26] M.I.A. Alzubaidi, A.S.A. Altawwash, W.N. Abbas, Study on the performance and emissions of compression ignition engine powered by diesel and biodiesel blends, Int. J. Thermofluids 24 (2024) 100869.

[27] S. Madhu, G.M. Lionus Leo, P. Prathap, Y. Devarajan, R. Jayabal, Effective utilization of waste pork fat as a potential alternate fuel in CRDI research diesel engine – Waste reduction and consumption technique, Process. Saf. Environ. Prot. 172 (2023) 815–824, https://doi.org/10.1016/j.psep.2023.02.057.

[28] M.E.M. Soudagar, et al., "Effect of variable compression ratio on the performance, combustion and emission characteristics of diesel engine: a review", SN. Appl. Sci. 2 (2) (2020) 1–12, https://doi.org/10.1007/s42452-020-2090-3.

[29] R. Dominguez-Faus, S.E. Powers, J.G. Burken, P.J. Alvarez, The water footprint of biofuels: a drink or drive issue? Env. Sci. Technol. 43 (9) (2009) 3005–3010, https://doi.org/10.1021/es802162x.

[30] A.F. Clarens, E.P. Resurreccion, M.A. White, L.M. Colosi, Environmental life cycle comparison of algae to other bioenergy feedstocks, Env. Sci. Technol. 44 (5) (2010) 1813–1819, https://doi.org/10.1021/es902838n.

[31] C.M. Starbuck, Comment on “environmental life cycle comparison of algae to other bioenergy feedstocks”, Env. Sci. Technol. 45 (2) (2010) 833, https://doi.org/10.1021/es103102s.

[32] E.P. Resurreccion, L.M. Colosi, M.A. White, A.F. Clarens, Comparison of algae cultivation methods for bioenergy production using a combined life cycle assessment and life cycle costing approach, Bioresour. Technol. 126 (2012) 298–306, https://doi.org/10.1016/j.biortech.2012.09.038.

[33] B. Halder, I. Ahmadianfar, S. Heddam, et al., Machine learning-based country-level annual air pollutants exploration using Sentinel-5P and Google Earth Engine, Sci. Rep. 13 (2023) 7968, https://doi.org/10.1038/s41598-023-34774-9.

[34] C. Sánchez, et al., "Design, synthesis, and properties of inorganic and hybrid thin films: a sol–gel solution", J. Mater. Chem. 21 (22) (2011) 8298–8312, https://doi.org/10.1016/j.jmatchem.2011.01.025.

[35] M.J.L. Santos, et al., "Life cycle assessment of TiO_2 nanoparticle synthesis: impact of solvent selection", J. Clean. Prod. 234 (2019) 545–555, https://doi.org/10.1016/j.jclepro.2019.06.235.

[36] F. Piccinno, et al., "Life cycle assessment of nanomaterials: state of the art and strategies to overcome barriers", Nano Today 7 (5) (2012) 409–429, https://doi.org/10.1016/j.nantod.2012.07.001.

[37] G. Jamuna, S. Yasodha, P. Thamarai, A.S. Vickram, S. Pavithra, A. Saravanan, P. R. Yaashikaa, Design strategies, utilization and applications of nano-engineered biomaterials for the enhancement of bioenergy: a sustainable approach, Biochem. Eng. J. 200 (2023) 109104, https://doi.org/10.1016/j.bej.2023.10910.

[38] G. Choubey, M. Solanki, O. Patel, W. Huang, Effect of different strut design on the mixing performance of H2 fueled two-strut based scramjet combustor, Fuel 351 (2023) 128972, https://doi.org/10.1016/j.fuel.2023.128972.

[39] Y. Devarajan, V.R. Madhavan, Emission analysis on the influence of ferrofluid on rice bran biodiesel, J. Chil. Chem. Soc. 62 (4) (2017) 3703–3707, https://doi.org/10.4067/s0717-97072017000403703.

[40] M.S. Gad, M.M.A. Aziz, H. Kayed, Impact of different nano additives on performance, combustion, emissions and exergetic analysis of a diesel engine using waste cooking oil biodiesel, Propuls. Power Res. 11 (2) (2022) 209–223.

[41] A. Gharehghani, H. Pourrahmani, Performance evaluation of diesel engines (PEDE) for a diesel-biodiesel fueled CI engine using nano-particles additive, Energy Convers. Manage. 198 (2019) 111921.

[42] J. Stevenson, Ecological assessments with algae: a review and synthesis, J. Phycol. 50 (3) (2014) 437–461, https://doi.org/10.1111/jpy.12189.

[43] B.R. Hosamani, S.A. Ali, V. Katti, Assessment of performance and exhaust emission quality of different compression ratio engine using two biodiesel mixture: artificial neural network approach, Alex. Eng. J. 60 (1) (2021) 837–844.

[44] Abdallah S. Elgharbawy, Ahmed I. Osman, Abdel Ghaffar M.El Demerdash, Wagih A. Sadikm, Mosaad A. Kasaby, Shimaa E. Ali, Enhancing biodiesel production efficiency with industrial waste-derived catalysts: techno-economic analysis of

microwave and ultrasonic transesterification methods, Energy Convers. Manage. 321 (2024) 118945, https://doi.org/10.1016/j.enconman.2024.118945.
[45] Rajendiran Naveenkumar, Gurunathan. Baskar, Optimization and techno-economic analysis of biodiesel production from Calophyllum inophyllum oil using heterogeneous nanocatalyst, Bioresour. Technol. 315 (2020) 123852, https://doi.org/10.1016/j.biortech.2020.123852.
[46] G. Choubey, P. Gaud, A. Mahmood Fatah, Numerical investigation on geometric sensitivity and flame stabilisation mechanism in H2 fueled two-strut based scramjet combustor, Fuel 312 (2022) 122847, https://doi.org/10.1016/j.fuel.2021.122847.